



Production of hydrogel microparticles in microfluidic devices: a review

A. Moreira¹ · J. Carneiro¹ · J. B. L. M. Campos¹ · J. M. Miranda¹

Received: 7 September 2020 / Accepted: 11 December 2020 / Published online: 14 January 2021
© The Author(s), under exclusive licence to Springer-Verlag GmbH, DE part of Springer Nature 2021

Abstract

Hydrogels are biocompatible materials commonly used in biological applications, such as cell encapsulation, tissue engineering and drug delivery systems. The use of hydrogels in the form of microparticles brings, for several purposes, many advantages, since the particles have a high surface-to-volume ratio and they can be delivered inside microscale structures such as blood microvessels and tissues. Microfluidic devices are a promising approach to produce hydrogel microparticles because they enable a high precision control of the flow streams during the microfabrication process, leading to microparticles with precise size, shape, mechanical properties and cross-linking density. In this review, the focus is put on the most important features to be considered when producing hydrogel microparticles through microfluidic devices. First, the design strategies of microfluidic devices, the selection of the operating conditions and the importance of surfactants are analyzed. Then, the most important gelation mechanisms are reviewed. Afterwards, the most commonly used hydrogel materials are introduced, and their properties are referred. Finally, the different methods to control the size, shape and particle microstructure are discussed and the main challenges for the future are addressed.

Keywords Hydrogels · Droplet microfluidics · Surfactants · Thermal gelation · Ionic gelation · Photopolymerization · Photolithography

Abbreviations

| | |
|-------------|---|
| PEG | Poly(ethylene glycol) |
| PEGDA | Poly(ethylene glycol) diacrylate |
| ELPs | Elastin-like peptides |
| PEO–PPO–PEO | Poly(ethylene oxide)–poly(propylene oxide)–poly(ethylene oxide) |
| PNIPAAm | Poly(N-isopropyl acrylamide) |
| PEGMEA | Poly(ethylene glycol) methyl ether acrylate |
| CFL | Continuous flow lithography |
| PDMS | Poly(dimethyl siloxane) |
| SFL | Stop flow lithography |
| SFIL | Stop flow interference lithography |
| SLMs | Spatial light modulators |
| DEP | Dielectrophoresis |
| EWOD | Electrowetting on dielectric |
| CMC | Critical micelle concentration |
| EDS | Equilibrium droplet size |

| | |
|-----|---------------------|
| PVA | Poly(vinyl alcohol) |
| HA | Hyaluronic acid |

List of symbols

| | |
|-----------|--|
| Ca_i | Capillary number of the phase i |
| μ_i | Viscosity of the phase i |
| v_i | Velocity of the phase i |
| σ | Surface tension between the two phases |
| Re_i | Reynolds number of the phase i |
| ρ_i | Density of the phase i |
| v_i | Velocity of the phase i |
| D | Diameter of the microchannel |
| φ | Flow rate ratio |
| Q_d | Flow rate of the dispersed phase |
| Q_c | Flow rate of the continuous phase |
| λ | Viscosity ratio |
| μ_c | Viscosity of the dispersed phase |
| μ_c | Viscosity of the continuous phase |
| We_i | Weber number of the phase i |
| Ca_c | Capillary number of the continuous phase |
| Ca_d | Capillary number of the dispersed phase |

✉ J. M. Miranda
jmiranda@fe.up.pt

¹ CEFT, Transport Phenomena Research Center, Chemical Engineering Department, Faculty of Engineering, University of Porto, 4200-465 Porto, Portugal

1 Introduction

Microparticles are used for cell encapsulation, medical imaging, drug delivery, biomolecule synthesis and diagnosis (Teh et al. 2008; Mazutis et al. 2015; Anna and Mayer 2006; Cubaud and Mason 2008), among other biomedical applications. To perform these roles, microparticles must be biocompatible, easy to produce and able to incorporate drugs or microorganisms (Tumarkin and Kumacheva 2009). These requirements can be easily met by hydrogels, due to the versatility of this family of materials (Tumarkin and Kumacheva (2009); Khademhosseini and Langer 2007; Zhang et al. 2016). Morphologically, hydrogels are cross-linked polymer networks that can contract or expand by releasing or absorbing water (Tumarkin and Kumacheva 2009). They change size in response to pH, temperature and ionic strength variations and their properties can be modified by introducing copolymers or other molecules in their network (Tumarkin and Kumacheva 2009). Hydrogels can be obtained through natural or synthetic resources, presenting in each case different characteristics (Tumarkin and Kumacheva 2009; Gao et al. 2012a).

Hydrogel microparticles can be produced by several methods, of which the most widespread are emulsification (Zamora-Mora et al. 2014a; Chuah et al. 2009), direct agitation and grinding of the polymer (Oliveira and Mano 2011), spray drying (Ré 2006) and microfluidics (Teh et al. 2008). Compared with the alternative methods, microfluidics has several unique advantages, as the size and shape of the microparticles can be accurately controlled enabling the manufacturing of monodispersed populations (Leng et al. 2010) with a large variety of shapes and compositions. Microfluidic devices are also suitable to control reaction, heat and mass transport rates, reducing waste and enabling the control of the characteristics of the microparticles. Furthermore, composite particles can be manufactured with precision and reproducibility combining different streams and using double-emulsion techniques or photolithography. The particle fabrication can be integrated with other components such as sensors, heaters, coolers, visualization windows and elements to conduct biological experiments. Finally, scaling up is possible through parallelization, which facilitates large-scale production.

The most straightforward method to produce hydrogel microparticles in microfluidic devices is droplet microfluidics. Microdroplets are produced using multiphase systems comprising a continuous phase (usually an oil), a dispersed phase (in this specific case, a hydrogel precursor) and a surfactant. To generate the droplets, the driving forces are the shear stress and the interfacial tension between phases. The surfactant is used to lower

the interfacial tension between the phases and to prevent coalescence of the droplets (Baret 2012; Baroud and Wilhelm 2004; Baret et al. 2009; Sharma et al. 2013; Xu et al. 2012). After formation, the microdroplets are solidified into hydrogel microparticles (gelation), inside or outside the channel, and through many different mechanisms depending on the hydrogel. The final size and shape of the microparticles depend on multiple parameters including the flow rates of the fluids, geometry, material composition and size of the channels and the fluid properties (Teh et al. 2008; Leng et al. 2010; Lee et al. 2009).

This review summarizes the different aspects of hydrogel microparticles production in microfluidic devices aiming to provide guidelines to select the operating conditions, the microfluidic device design and the selection of precursor fluids and carrier phases. Among the wide set of hydrogels available, the most commonly produced in microfluidic devices are agarose, alginate and poly(ethylene glycol)—PEG. These hydrogels will be analyzed in more detail. The design of microfluidic devices is analyzed in Sect. 2 and the role of surfactants in hydrogel particle formation is described in Sect. 3. Hydrogels have different gelation mechanisms, which have implications on the design of the microfluidic devices to produce microparticles. The gelation mechanisms are discussed in Sect. 4: thermal gelation (Tumarkin and Kumacheva 2009; Jagur-Grodzinski 2009), ionic gelation (Patil et al. 2010, 2012; Patel et al. 2017; Sacco et al. 2016) and photopolymerization (Nguyen and West 2002). The properties of some hydrogel precursors and hydrogel particles are summarized in Sect. 5. The size, accuracy and shape restrictions of each fabrication method are discussed in Sect. 6. The challenges for the future are addressed in Sect. 7, with emphasis on the development of high-throughput particle production.

2 Microfluidic systems

Microfluidic technologies offer efficient methods to produce highly monodispersed microparticles of new materials, which are applicable in different fields such as biology, medicine and chemistry (Teh et al. 2008; Mazutis et al. 2015; Anna and Mayer 2006; Christopher and Anna 2007). There are many options to produce and manipulate droplets, namely through: dielectrophoresis (DEP) -driven droplet generation (Yang et al. 2010), electrowetting on dielectric (EWOD) -driven droplet generation (Yang et al. 2010), electrohydrodynamic manipulation (Yang et al. 2010), thermocapillary manipulation (Yang et al. 2010; Baroud et al. 2007; Darhuber et al. 2003; Chen et al. 2005; Gao et al. 2012b), magnetic actuation (Yang et al. 2010; Yizhong et al. 2007; Todd and Jon 2013; Tsuchiya et al. 2008; Say-Hwa et al. 2010; Zhang and Nguyen 2017), acoustic actuation

(Yang et al. 2010; Wixforth et al. 2004; Oberti et al. 2009; Destgeer and Sung 2015) and hydrodynamic manipulation (Teh et al. 2008; Yang et al. 2010; Yizhong et al. 2007; Pethig 2010; Jones et al. 2001; Wehking et al. 2013; Nelson and Kim 2012; Sung Kwon et al. 2003; Gong and Kim 2008). Although all these techniques are very important in the production and manipulation of droplets, hydrodynamic methods are the most commonly used, so they get more attention in the following sections.

2.1 Droplet production

Hydrodynamic droplet production techniques take advantage of shear and interfacial forces to generate droplets (Leng et al. 2010). The production rate, size and shape of the droplets are mostly dependent on the flow rates, physical properties of the phases and geometry/design/material of the channels (Teh et al. 2008; Leng et al. 2010; Lee et al. 2009).

The channels used in hydrodynamic manipulation are usually made in PDMS—poly(dimethylsiloxane)—due to the low-cost fabrication process and easy control of the surface chemistry (Duffy et al. 1998; McDonald and Whitesides 2002). Although with these advantages over other materials, PDMS swells or degrades when exposed to some solvents (Lee et al. 2003). Other materials that can be used to replace PDMS are glass, silicon and thiolene (Teh et al. 2008; Christopher and Anna 2007; Lee et al. 2003). Methods to fabricate PDMS microfluidic devices have been described in detail by Duffy et al. (1998),

McDonald and Whitesides (2002), Mata et al. (2005) and McDonald et al. (2000), while detailed information on solvent selection is available in Lee et al. (2003) work. The most common microfabrication technique for the production of PDMS channels is based on planar photolithography, for the production of SU-8 molds (Campo and Greiner 2007; Lorenz et al. 1997; Natarajan et al. 2008), and soft lithography for the production of the channels from the molds (Friend and Yeo 2010). Using these techniques, the characteristic size of the channels can be smaller than $2\ \mu\text{m}$ (Campo and Greiner 2007). Alternatively, the community working on droplet microfluidics also uses capillary tubing devices (Jeong and Kim 2011; Utada et al. 2005; Martinez et al. 2012).

To produce microdroplets by hydrodynamic manipulation, the most common designs are T-junction, co-flow and flow-focusing geometries (Christopher and Anna 2007). In a T-junction configuration (Fig. 1a), the continuous phase, which flows in the main channel, is intersected by the dispersed phase, which flows in a secondary channel. In a flow-focusing configuration (Fig. 1b), the flow of the dispersed phase in the main channel is squeezed by the flow of the continuous phase entering by two lateral channels (Samipour et al. 2016; Xu et al. 2009). A configuration similar to the flow-focusing configuration is the co-flow configuration (Fig. 1c), in which the dispersed and continuous phases flow in the same direction in parallel microchannels (Christopher and Anna 2007; Yang et al. 2010); in the inner flows the dispersed phase and in the outer the continuous phase.

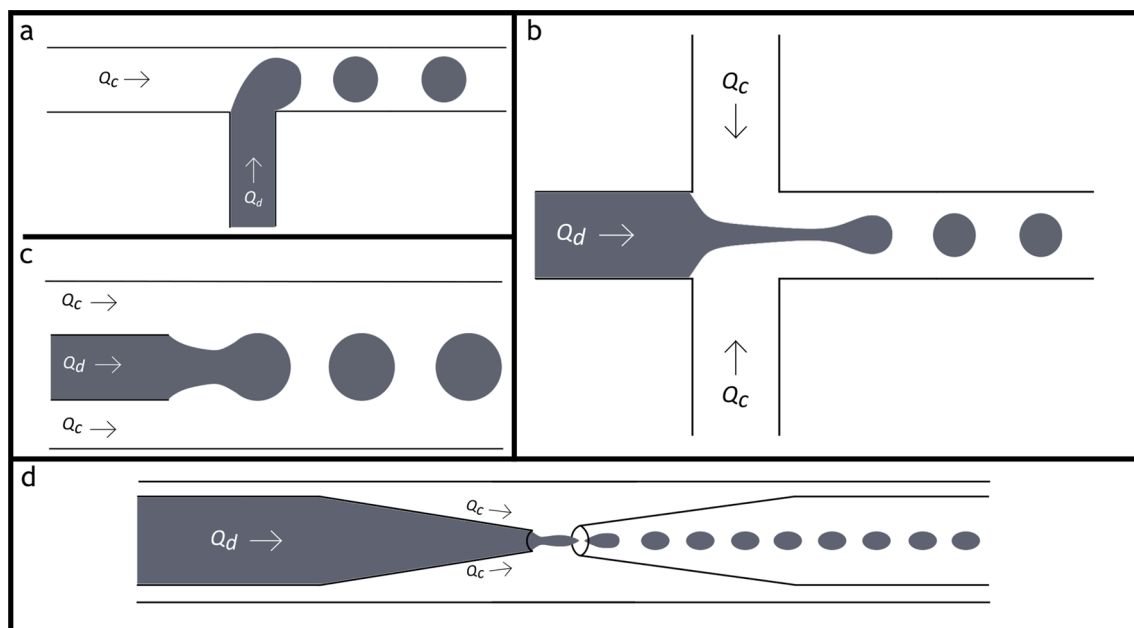


Fig. 1 Designs commonly used in droplet microfluidics: **a** T-junction scheme; **b** flow-focusing scheme; **c** Co-flow scheme; **d** droplet formation using capillaries

As aforementioned, microcapillary tubing is another approach to fabricate microchannels for droplet microfluidics (Jeong and Kim 2011; Utada et al. 2005; Martinez et al. 2012). A typical configuration is shown in Fig. 1d. Two tapered capillaries are inserted, pointing each other, inside a squared capillary. One of the tapered capillaries is the inlet of the dispersed phase and the other is the outlet that collects the droplets. The continuous phase flows in the space between the inlet microcapillary and the squared capillary.

The size of the droplets formed depends on the fluids viscosity and density, surface tension, flow rates and surface properties and geometry of the device (Teh et al. 2008; Choi et al. 2007). Dimensional analysis leads to a correlation between the non-dimensional size of the droplets and Capillary (Ca_d) and Reynolds (Re_c) numbers of each phase, viscosity ratio (λ) and contact angle. Alternatively, one of the Capillary numbers can be replaced by the flow rate ratio (ϕ). Typical flows in microfluidic systems are characterized by very low Reynolds numbers; viscous forces are dominant and no significant flow variations are observed when the Reynolds number changes (Teh et al. 2008; Lee et al. 2009; Yang et al. 2010). Only in high-speed flows, the inertial forces become significant and the Reynolds number effects should then be taken into account (Baroud et al. 2010).

In droplet formation, the flow patterns are influenced by the aforementioned dimensionless numbers. To visualize this dependence, the data from experiments are usually represented in regime maps. A typical regime map displays the regimes in two-dimensional diagrams like the one represented in Fig. 2. In this diagram, the coordinates are the

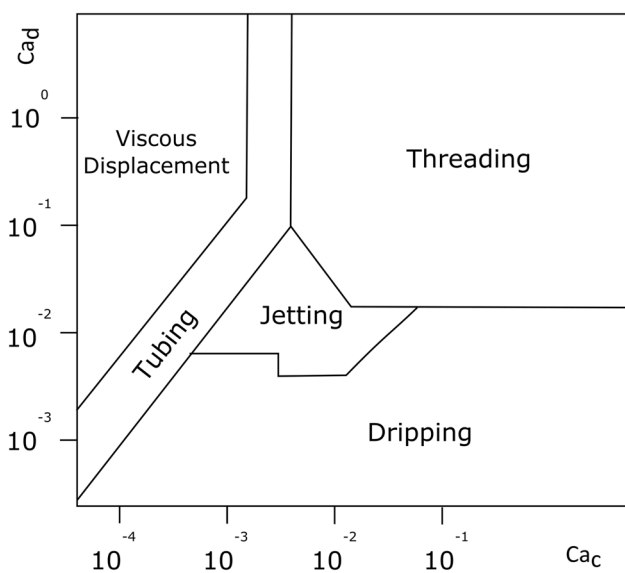


Fig. 2 Scheme of a flow map regimes for a flow-focusing device—based on Cubaud and Mason (2008). Each flow map regime is valid for a viscosity ratio

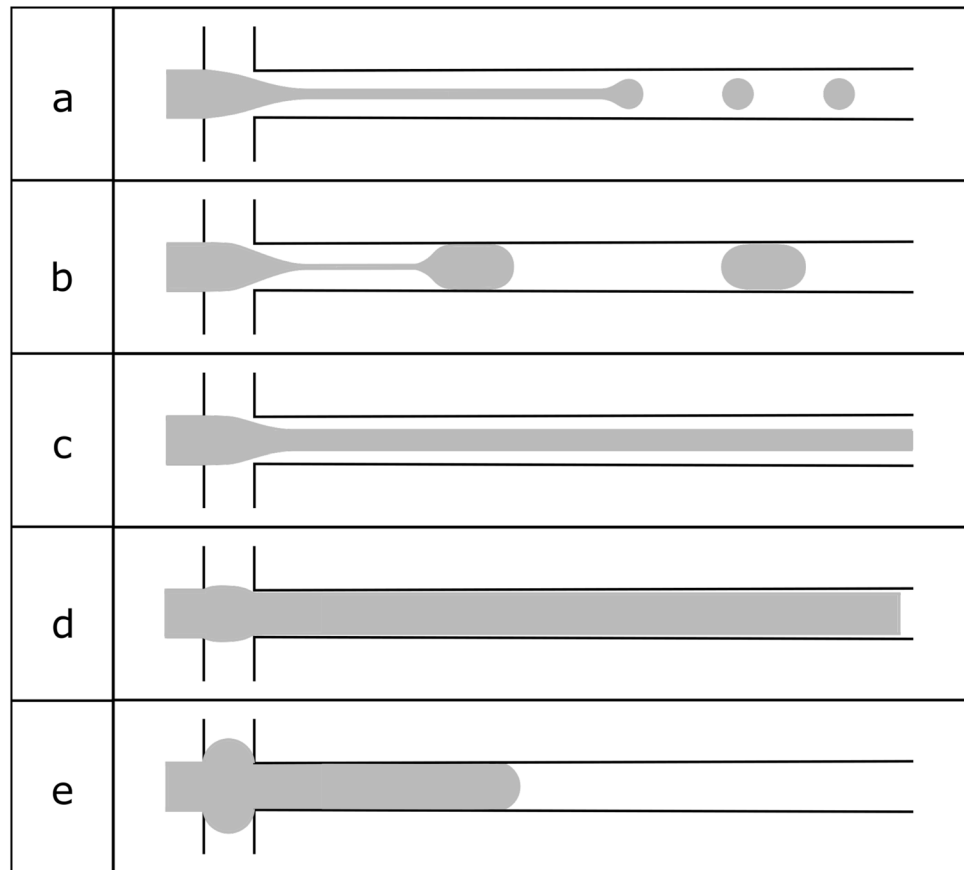
Capillary numbers. The regime map is valid for a given viscosity ratio.

In a flow-focusing device, the most commonly observed flow patterns are: jetting, dripping, threading, tubing and viscous displacement (Cubaud and Mason 2008; Carneiro et al. 2016). In the jetting regime, Fig. 3a, the thread of the dispersed phase breaks far from the focusing section. In the dripping regime, Fig. 3b, the thread of the dispersed phase breaks and retracts, leading to the formation of a droplet near the focusing section. When the thread is stable and does not break, a threading pattern is observed—Fig. 3c. Tubing (Fig. 3d) is similar to threading, but, in this case, the dispersed phase fills almost all the cross-section of the main channel. When the flow rates ratio is too high, the dispersed phase starts to invade the inlet channels of the continuous phase, leading to viscous displacement regime—Fig. 3e. Two additional flow patterns have been referred in the literature for $Ca_d < 10^{-3}$ and $Ca_c > 0.3$: tip streaming (Anna and Mayer 2006; Jeong et al. 2012) and tip-multi-breaking (Zhu et al. 2015).

To produce hydrogel particles with specified characteristics, some tools are required to predict the flow regime, the polydispersity and particle size. Microdroplets are generated only in the dripping and jetting regimes and the regime map shows the ranges of Capillary numbers where those regimes lie (Carneiro et al. 2016). Polydispersity is directly related to the flow regime. Carneiro et al. (2016) characterized PDMS droplet formation in a microfluidic flow-focusing device and concluded that the best flow conditions to obtain monodisperse microdroplets are the dripping regime. The particle size trends can be analyzed through the equations of Cubaud and Mason (2008). These authors developed and tested predictive equations for the size of the droplets in the dripping and jetting regimes for systems without surfactants.

The analysis of particle size trends is not a simple matter, since size trends are geometry dependent and interplay with regime changes, as shown by the results of several papers in the literature. For example, Dang et al. (2012) produced monodisperse PEG microparticles in a flow-focusing device and observed a decrease in the size of the droplets with the increase of the continuous phase flow rate, behavior consistent with the trend predicted by Cubaud and Mason (2008). Dang et al. (2012) also observed that high concentrations of PEG induce large microdroplets. Since multiple factors are involved, the explanation of this effect is not straightforward. Concentrated PEG solutions have high viscosity and high surface tension, being the viscosity increase dominant. For this reason, high concentrations lead to high Capillary numbers of the dispersed phase. Carneiro et al. (2016) PDMS data show that the effect of the Capillary number of the dispersed phase on the droplet size is non-monotonic and depends on the flow regime. As Dang et al. (2012) did not characterize the flow regime, their findings cannot be

Fig. 3 Scheme of different flow regimes in a flow-focusing device: **a** jetting, **b** dripping, **c** threading, **d** tubing, **e** viscous displacement



checked in more detail. Furthermore, they used non-standard geometry and geometrical effects alone may explain the observed increase of the particle size with concentration. This emphasizes the importance of the regime map for the specific experimental conditions used.

Hydrodynamic droplet formation is a passive method that relies on the use of syringe pumps to control the flow rates and on geometrical constrictions of the microdevice. It is not always possible to produce droplets of the desired size because the ranges of flows and control precision required are not achievable using syringe pumps. Active methods based on acoustic actuation (Brenker et al. 2016; Schmid and Franke 2014) have been used to circumvent some of the limitations of the hydrodynamic methods, such as size and size distribution limitations. Acoustic actuation based on surface acoustic waves has smaller capacitive effects, and thus are suitable to precisely control droplet formation and to obtain very small droplets.

2.2 Droplet manipulation

Microfluidic techniques enable the production of highly monodispersed droplets and each one of these droplets can serve as a base for chemical reactions or cell encapsulation (Teh et al. 2008). Procedures such as droplet fission,

droplet fusion and droplet sorting may be required during the fabrication and encapsulation processes. Sequential droplet fission can help to scale-up droplet formation (Teh et al. 2008) and can be attained by passive or active methods. The passive methods consist of using the shear forces that are created by specific designs of the microchannels to split the droplets, such as T-junctions, channels with branches or with obstructions (Teh et al. 2008; Sharma et al. 2013; Yang et al. 2010; Cerdeira et al. 2020). Active methods use external power or electrical forces to split the droplets (e.g., EWOD) (Teh et al. 2008). Through droplet fusion (Teh et al. 2008; Sharma et al. 2013), it is also possible to merge the droplets, creating droplets with larger diameters. This procedure is useful in particle production to enable reaction control. The passive methods consist on the use of a specific microchannel design to control the fusion in a certain location, such as a channel junction, an obstruction or an expanded region in the microchannel (Teh et al. 2008; Yang et al. 2010). Drop fusion can also be promoted by active methods, like EWOD or other techniques that require electrical forces (Teh et al. 2008; Sharma et al. 2013).

Sorting of droplets can also be interesting for the study of isolated droplets, purification of droplets and control of polydispersed droplet mixtures (Teh et al. 2008). The sorting of the droplets can be promoted using a channel geometry

based on the size of the droplets or using the gravitational force (Teh et al. 2008; Yang et al. 2010). Electrical forces can also be employed to sort the droplets. EWOD and DEP are two of the techniques used to sort the droplets (Teh et al. 2008; Sharma et al. 2013).

3 Surfactants

Despite the several advantages of the microfluidic systems to produce hydrogel microparticles, droplet coalescence can arise before gelation, becoming a problem for particle production. To stabilize the droplet emulsion, prevent coalescence and stabilize the droplet interface, surfactants must be added to one of the phases. Surfactants are amphiphilic molecules that modify the properties of interfaces. Amphiphilic molecules have two different functional groups, usually hydrophilic and oleophilic groups (Baret 2012; Baroud and Willaime 2004). For this reason, the surfactant is driven to the interface, reducing the interfacial tension (Baret 2012; Xu et al. 2012; Mazutis and Griffiths 2012). The interfacial tension reaches its lowest value at the critical micelle concentration (CMC) (Tostado et al. 2011), which is a characteristic of the surfactant. Above the critical concentration, the additional surfactant molecules form micelles (Farn 2008) and the interfacial tension is constant (Tostado et al. 2011; Myers 2005). The surfactant can also modify the rheology of the interface (Fischer and Erni 2007) (its viscosity and elasticity), which has an impact on the particle size. This effect is usually difficult to analyze since data are scarce and interface rheology requires specialized equipment unavailable in most laboratories.

Furthermore, the distribution of surfactant in the flow is significantly influenced by mass transport limitations, which hinder droplet formation and stability. Coalescence can persist if the adsorption time of the surfactant into the interface is longer than the formation time of a new droplet (Baret 2012; Baret et al. 2009; Xu et al. 2012). However, mass

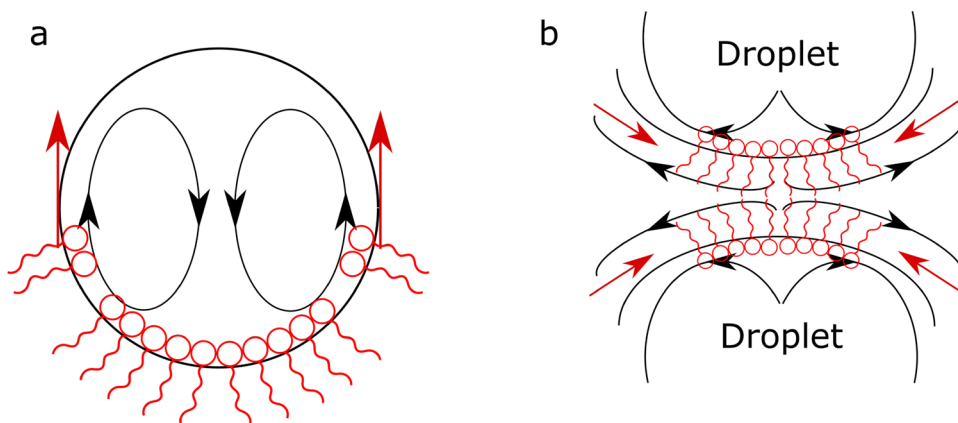
transport limitations can also contribute to droplet stability. When the distribution of the surfactant at the surface of the droplet is not uniform and a concentration gradient is created, a stress opposed to the flow direction can be generated rigidifying the interface; this is called the Marangoni effect—Fig. 4. Marangoni forces can impact the flow around the interface of the droplet (Baret 2012; Xu et al. 2012) and hinder coalescence. The Marangoni effect can also influence droplet size, as shown in the work of Xu et al. (2012).

Another effect that can be observed in microfluidic droplet generation is the Ostwald ripening effect, which is characterized by the growth of large droplets (McClements et al. 2012; Wooster et al. 2008), due to the coalescence of small ones (McClements et al. 2012; Wooster et al. 2008). This effect is induced by the higher Laplace pressure in the smaller droplets leading to their dissolution in the bigger ones, (Baret 2012). The Ostwald ripening effect can be avoided by adding hydrophobic molecules to the continuous phase (McClements et al. 2012).

Figure 5, based on information from Baret (2012), shows combinations of hydrocarbon oils/surfactants that can be used for several applications. In the formation of hydrogel droplets in microfluidics, the most used surfactant is Span 80. Span 80 is a non-ionic surfactant that can be used together with different hydrocarbon oils, such as hexadecane, mineral oil, rapeseed oil and kerosene (Baret 2012). It is largely used in the pharmaceutical industry due to its properties and effects in emulsions at low concentrations (Pensado et al. 2014). Span 80 is used in microfluidics with two purposes: decrease the interfacial tension between phases and to form a protective coat around the droplets to avoid coalescence (Benmekhbi et al. 2014). Park et al. (2016) used Span 80 to prevent the coalescence of gelatin droplets (Fig. 6a) and Zamora-Mora et al. (2014a) used Span 80 to obtain the same effect in cooperative hydrogels of chitosan/agarose—Fig. 6b and c.

A few experimental reports have analyzed the effect of the surfactant on droplet formation. (Choi et al. 2007)

Fig. 4 Marangoni effect: **a** in the presence of surfactant, the flow induces a concentration distribution of surfactant around the droplet causing a stress opposed to the flow direction (Marangoni stress—red arrows); **b** Marangoni stresses act against the film avoiding coalescence



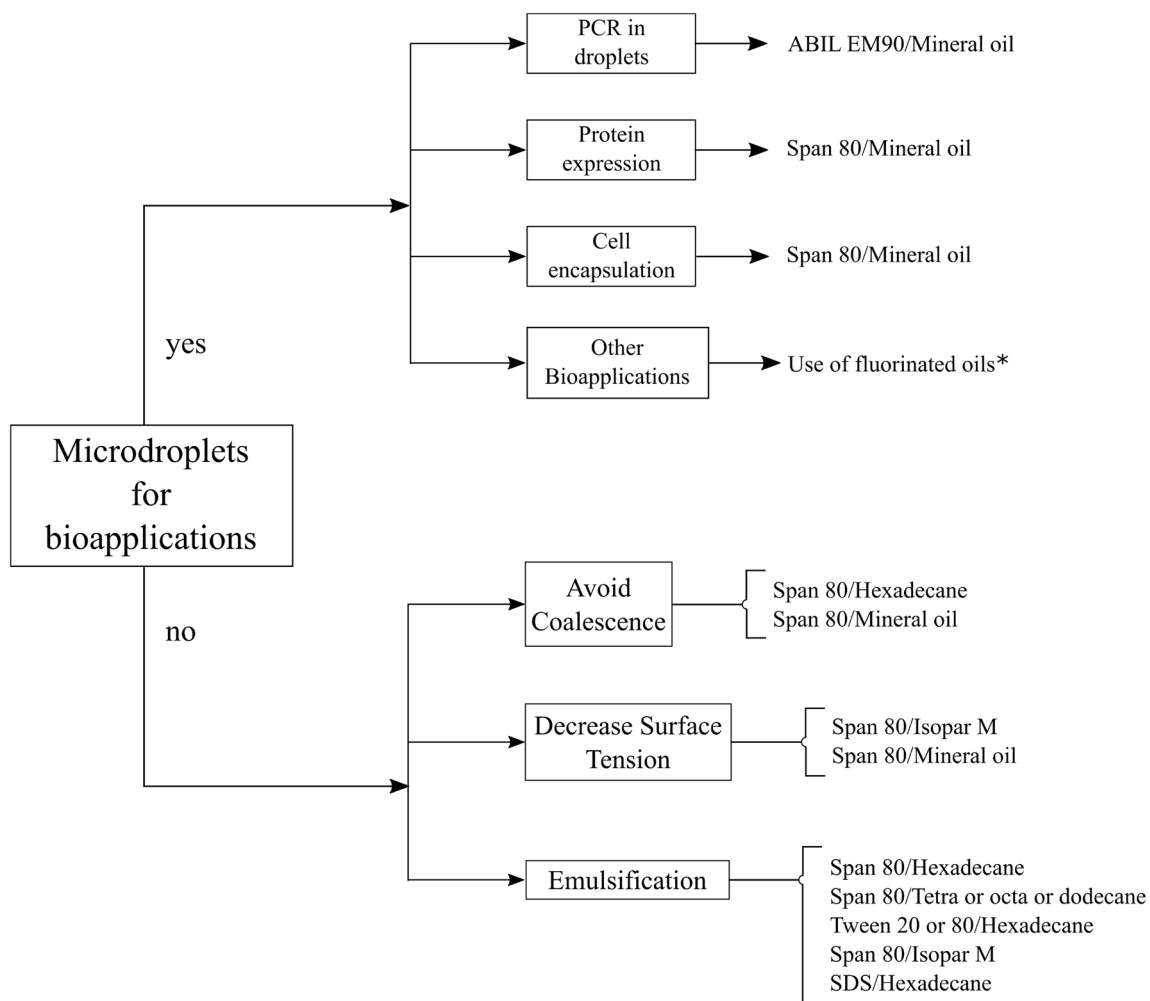


Fig. 5 Guide for the selection of the continuous phase and surfactants for different applications [based on information from Baret (2012)]. Please take note that some substances can affect the PDMS performance (Lee et al. 2003)

produced monodispersed droplets of alginate using Span 80 as a surfactant—Fig. 7a. They concluded that the size of the droplets decreases with increasing concentration of Span 80. Choi et al. (2009) produced monodispersed microspheres of PEGDA using a flow-focusing device—Fig. 8 a and b. They found that the surfactant concentration must be above 3%, otherwise the interfacial tension is too high and the microdroplets formed have an irregular shape. They also concluded that when the concentration of the surfactant increases, the size of the droplets decreases. These results are consistent with the observation by Cubaud and Mason (2008) that the droplet size decreases with the increase of the Capillary number of the continuous phase. They are also consistent with the results obtained by Xu et al. (2012).

Capillary numbers are inversely proportional to the interfacial tension between phases and so, according to Fig. 2, the surfactant plays an important role in droplet formation. When the surfactant concentration increases, the interfacial

tension decreases leading to higher Capillary numbers. The increase of the Capillary number of the continuous phase leads to smaller droplets, while the effect of increasing the Capillary number of the dispersed phase is dependent on the flow regime. If the regime changes from dripping to jetting, sub-channel size particles can be obtained. The surfactant can also change the Capillary number through an alteration of the viscosity.

4 Gelation mechanisms

The most common gelation methods are thermal gelation, ionic gelation and photopolymerization. Each of these methods has specific requirements with implications on the design and operation of the devices. The gelation mechanism usually requires heating or cooling systems, channels

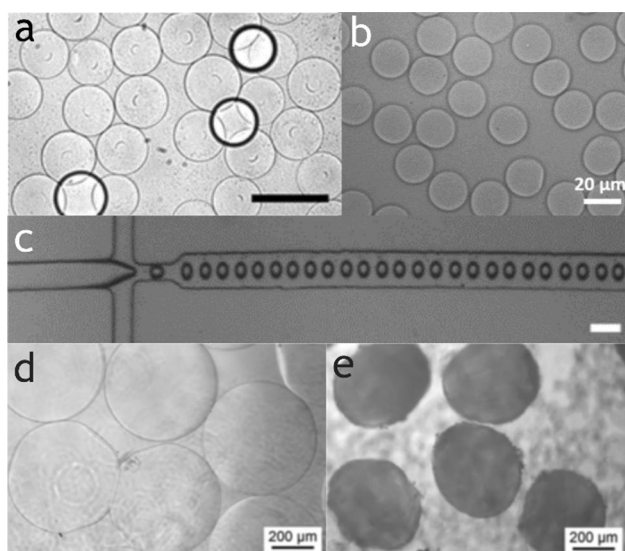


Fig. 6 Microparticles and microdroplets obtained by thermal gelation: **a** optical microscopy of gelatine hydrogel microspheres suspended in water—Adapted by permission from Springer Nature, Macromolecular Research, Synthesis and characterization of thermosensitive gelatin hydrogel microspheres in a microfluidic system, (Park et al. 2016). Copyright 2020. Scale bar=100 µm. **b** Optical microscopy image of chitosan/agarose in PBS buffer at 25 °C; and **c** optical microscopy images of the chitosan/agarose droplets. Scale bar=70 µm. Reprinted from Carbohydrate Polymers, Vol 111, (Zamora-Mora et al. 2014b), chitosan/agarose hydrogels: cooperative properties and microfluidic preparation, Copyright 2020, with permission from Elsevier. doi.org/10.1016/j.carbpol.2014.04.087. **d** Warm droplets of agarose and **e** lyophilized microparticles of agarose—Reprinted from Acta Biomaterialia, Vol 12, Agarose particle-templated porous bacterial cellulose and its application in cartilage growth in vitro, (Yin et al. 2015). Copyt 2020, with permission from Elsevier. doi.org/10.1016/j.actbio.2014.10.019

to deliver specific reactants, waveguides or optical windows for UV light sources.

4.1 Thermal gelation

Thermal gelation is a physical cross-linking method (Tumarkin and Kumacheva 2009; Jagur-Grodzinski 2009; Pochan et al. 2003; Cellesi et al. 2004; Hoare and Kohane 2008) induced by hydrophobic interactions, hydrogen bonding or ionic interactions caused by temperature changes in the polymeric solution (Tumarkin and Kumacheva 2009; Jagur-Grodzinski 2009). The gelation temperature depends on the concentration and chemical structure of the polymer (Hoare and Kohane 2008; Huang et al. 2013). Since gelation is reverted when the temperature is set back (Jagur-Grodzinski 2009; Jo et al. 2006), hydrogels that undergo thermal gelation (Huang et al. 2013) are usually called thermoreversible hydrogels. Examples of microparticles produced by thermal gelation can be found in Fig. 6.

Thermal gelation can be triggered upon cooling (Pochan et al. 2003; Joo et al. 2007; Klouda and Mikos 2008; Park et al. 2011) or heating (Pochan et al. 2003; Joo et al. 2007; Klouda and Mikos 2008; Park et al. 2011) of the hydrogel precursor. Materials that change from liquid to gel form upon cooling include agarose, kappa-carrageenan, poly(vinyl alcohol)—PVA and gelatin (Jo et al. 2006; Klouda and Mikos 2008; Nishinari and Watase 1987; Petka et al. 1998; Liu et al. 2010). Materials that undergo gelation by heating include elastin-like peptides (ELPs), Pluronics, block and star copolymers of PEG and poly(N-isopropyl acrylamide) and cellulose derivatives (Gao et al. 2012a; Hoare and Kohane 2008; Klouda and Mikos 2008; Petka

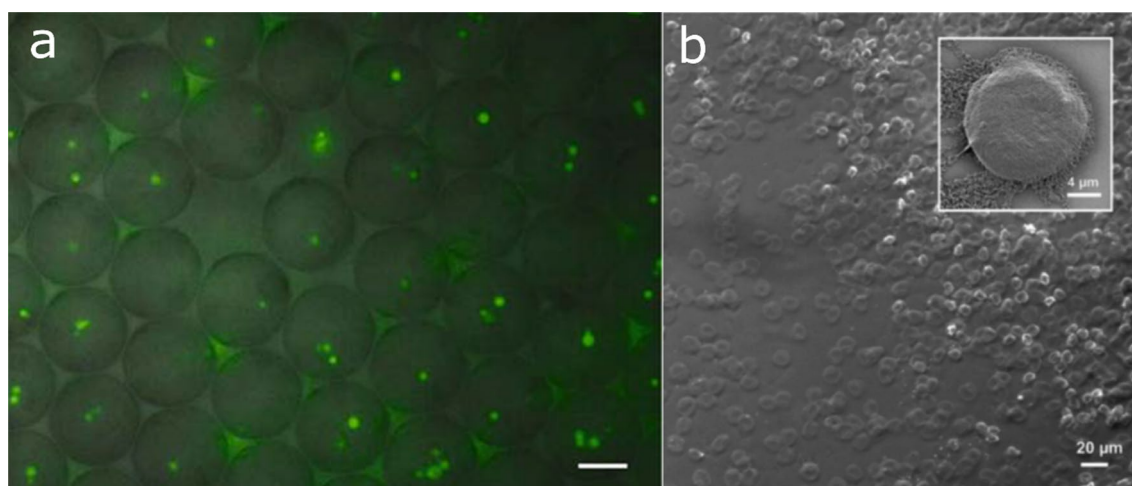


Fig. 7 Alginate microparticles. **a** Encapsulation of GFP-yeast cell into alginate microbeads—Adapted by permission from Springer Nature, Biomedical microdevices, Generation of monodisperse alginate microbeads and in situ encapsulation of cell in microfluidic device (Choi et al. 2007). Copy 2020. Scale bar=50 µm. **b** Algi-

nate microparticles with biconcave shape produced in a microfluidic chip—Reprinted from John Wiley and Sons, Macromolecular Bioscience, Microfluidic Production of Alginate Hydrogel Particles for Antibody Encapsulation and Release (Mazutis et al. 2015), © 2015 WILEY-VCH Verlag GmbH & Co. KGaA, Weinheim

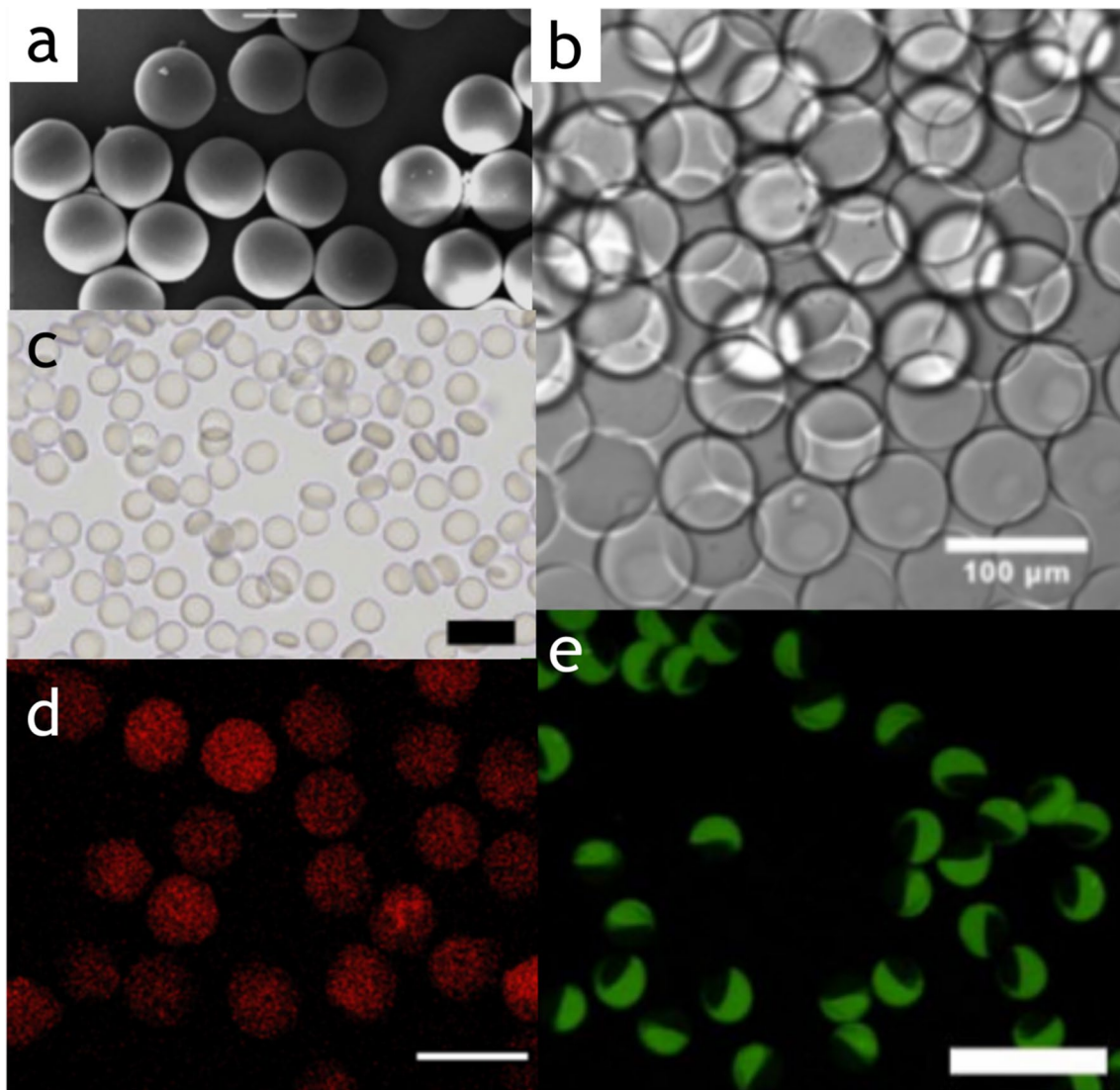


Fig. 8 Microparticles obtained by photopolymerization. **a** Optical microscopy image of the monodispersed PEG microspheres suspended in hexadecane; and **b** SEM image of PEG microspheres. Scale bar=100 μm . Adapted by permission from Springer Nature, Macromolecular Research, In situ microfluidic synthesis of monodisperse PEG microspheres, (Choi et al. 2009). Copyright 2020. **c** Microparticles of PEGDA containing fluorescently labeled TMV nanotemplates—Adapted with permission from (Lewis et al. 2010). Copyright 2020 American Chemical Society. Scale bar=100 μm . **d** Optical

image of encapsulated *E. coli* in PEG microbeads—Adapted by permission from Springer Nature, Macromolecular Research, Synthesis and utilization of *E. coli*-encapsulated PEG-based microdroplet using a microfluidic chip for biological application, (Lee et al. 2010a). Copyright 2020. Scale bar=100 μm . **e** Fluorescence micrographs of PEGDA Janus microparticles with one side of the particles containing fluorescently labeled TMV—Adapted with permission from (Lewis et al. 2010). Copyright 2020 American Chemical Society. Scale bar=100 μm

et al. 1998; Lin and Cheng 2001; Weng et al. 2004; Ahmadi and Bruijn 2008).

Thermoreversible hydrogels do not require chemical reactions, cross-linkers or UV irradiation. Thus, thermoreversible hydrogels are usually biocompatible, biodegradable and have low toxicity (Tumarkin and Kumacheva 2009; Jagur-Grodzinski 2009). Due to these characteristics, thermal gelation can be used to produce biocompatible microparticles for biomedical purposes. For example, Yin et al. (2015) incorporated monodispersed agarose microparticles,

thermally treated, in the fabrication of porous bacterial cellulose (pBCs) scaffolds for in vitro cell culture—Fig. 6d and e. They used a microfluidic device to control the dimensions and the monodispersity of the microparticles.

To produce microparticles by thermal gelation in microfluidic devices by droplet microfluidics (Table 1), the experimental setups require temperature control systems at different steps of the process (Tumarkin and Kumacheva 2009). This problem has been solved by operating the device in a temperature-controlled room or chamber, moving the

Table 1 Production of thermoreversible microparticles in microfluidic devices

| Hydrogel | Continuous phase | Surfactant | Size | Channel width | References |
|------------------|--------------------------|-------------------|------------------------------|-------------------|----------------------------|
| Agarose | Mineral oil and glycerol | Span 80 (3% wt) | 110 μm | 20 μm | (Kumachev et al. 2011) |
| Agarose | Oil | – | 180 \pm 7 μm | 360 μm | (Leng et al. 2010) |
| Chitosan/agarose | Mineral oil | Span 80 (3% w/v) | 18.4 \pm 2.3 μm | 70 μm | (Zamora-Mora et al. 2014a) |
| Agarose | Mineral oil | – | 300–500 μm | 889 μm | (Yin et al. 2015) |
| Gelatine | Soybean oil | – | 45–120 μm | 100 μm | (Yeh et al. 2013) |
| Gelatine | Mineral oil | Span 80 (20% w/w) | 66 μm | 54 μm | (Park et al. 2016) |
| Gelatine | Rapeseed oil | – | 115–160 μm | 20 μm | (Wassén et al. 2012) |
| Gelatine | Liquid parafin | – | 200 μm | 300 μm | (Sakai et al. 2011) |
| K-carrageenan | Palm oil | – | 0.76 mm | 0.55 mm | (Leong et al. 2011) |
| K-carrageenan | Palm oil | – | 1.3–1.8 mm | 0.8 mm | (Jegannathan et al. 2009) |

droplets between controlled environments at different temperatures (Aubry et al. 2015) or, the ideal choice, by adding heating elements to the microdevice (Yeh et al. 2013). An example of a microfluidic device with an integrated heating element was developed by Yeh et al. (2013). The heating element consists of an indium thin oxide (ITO) electrode controlled by an imposed voltage. The temperature was monitored near the droplet formation and kept at 95 °C.

4.2 Ionic gelation

Ionic gelation is the cross-linking of polyelectrolyte polymer solutions by counter ions induced by a specific condition, such as pH (Patil et al. 2010, 2012; Patel et al. 2017; Sacco et al. 2016). Several hydrogels can form a gel in the

presence of ions. The most commonly used in microfluidics are sodium alginate (Table 2), chitosan and gellan gum. Sodium alginate is soluble in water, however, in contact with divalent or polycations forms an insoluble solid structure (Patil et al. 2010, 2012; Patel et al. 2017; Leong et al. 2016). The most used ions to cross-link sodium alginate are calcium and zinc (Patil et al. 2010, 2012; Sacco et al. 2016; Leong et al. 2016). Chitosan is cross-linked with poly-anions, such as alginates (Patil et al. 2010, 2012; Perez Bravo and Francois 2016). Gellan gum can be cross-linked with mono- or divalent cations and carboxymethyl cellulose derivatives are usually cross-linked with metal ions (Patil et al. 2010, 2012).

Ionic gelation can arise through several different mechanisms: external gelation, internal gelation, inverse gelation, interfacial gelation and multi-step interrupted gelation

Table 2 Production of alginate microparticles in microfluidic devices

| Cross-linker | Cont. phase | Surfactant | Method | Size | Channel width | Ref |
|---------------------------------|------------------------|---------------------------------|---------------------------------|-----------------------|-------------------|------------------------------|
| Calcium chloride | N-Hexadecane | Span 80 (1 wt%) | On-chip coalescence of droplets | 60–95 μm | 90 μm | (Choi et al. 2007) |
| | Food oil | – | On-chip coalescence of droplets | 104–167 μm | 50 μm | (Shintaku et al. 2006) |
| | FC 40 carrier oil | Fluorinated surfactant (3% w/w) | On-chip coalescence of droplets | 10 μm | 10 μm | (Mazutis et al. 2015) |
| | Mineral oil | Span 80 (0.5% w/w) | On-chip coalescence of droplets | 107 μm | 50 μm | (Um et al. 2008) |
| | Mineral oil | Span 80 (0.4% w/w) | On-chip coalescence of droplets | 60–230 μm | 40 μm | (Martinez et al. 2012) |
| | Mineral oil | – | On-chip coalescence of droplets | 41.2 μm | 50 μm | (Liu et al. 2012) |
| | Octyl alcohol oil | – | On-chip internal gelation | 50–300 μm | 130 μm | (Xu et al. 2008) |
| | Soybean oil | – | On-chip coalescence of droplets | 41.3 μm | 50 μm | (Liu et al. 2006) |
| CaCO ₃ nanoparticles | Corn oil + acetic acid | Tween 20 (0.1% w/w) | On-chip internal gelation | 94–112 μm | 50 μm | (Tan and Takeuchi 2007) |
| | Fluorocarbon oil | Fluorinated surfactant (1% w/w) | On-chip internal gelation | 26 μm | 20 μm | (Akbari and Pirbodaghi 2013) |

(Leong et al. 2016). The most commonly used mechanisms in microfluidics are internal gelation and external gelation, therefore they will be described in more detail.

In external gelation, the droplets of the pre-polymer solution are surrounded by ions introduced in the continuous phase of the microfluidic device. Afterwards, the ions start to cross-link and the interface of the droplet turns into solid (Tumarkin and Kumacheva 2009; Leong et al. 2016); a solid shell and a liquid core are then formed. In the literature, the simplest procedure to carry out external gelation is to promote the contact between the formed droplets and the ions off-chip, in a bath containing ions (Tumarkin and Kumacheva 2009; Leong et al. 2016). External gelation can also be conducted on-chip, but care must be taken to assure that gelation does not start before droplet formation. This requirement led to the development of several new chip designs (Fig. 9b–d) and mixing strategies, including the mixing of the pre-polymer and the cross-linker in the region of droplet formation (Choi et al. 2007), the fusion of droplets containing the cross-linker with droplets containing the pre-polymer (Liu et al. 2006, 2012; Shintaku et al. 2006) and the use of a third fluid layer to delay the diffusion of the cross-linker to the region containing the pre-polymer (Mazutis et al. 2015; Xu et al. 2008).

In internal gelation, gelation is induced by a trigger external to the droplet (Leong et al. 2016). The cross-linker is

initially in an inactive state within the droplet and is activated by an external factor, releasing ions (Leong et al. 2016), which start to cross-link the droplet. Internal gelation of alginate can be induced on-chip or off-chip. In both cases, droplets containing CaCO_3 nanoparticles and alginate are formed and afterwards get in contact with a low pH phase that induces the release of Ca^{2+} from the nanoparticles leading to gelation (Fig. 9a).

4.3 Photopolymerization

Photopolymerization is induced by UV radiation in the presence of a photoinitiator. The UV light interacts with the photoinitiator originating free radicals which polymerize forming a cross-linked hydrogel (Nguyen and West 2002). Photopolymerization facilitates the temporal and spatial control of the polymerization, induces fast curing rates and can be conducted at room or physiological temperature (Nguyen and West 2002). Hydrogels that undergo photopolymerization include PEG derivatives, PVA derivatives and hyaluronic acid derivatives.

The simplest approach to produce microparticles by photopolymerization is by combining droplet microfluidics with UV radiation to solidify the droplets (Table 3). For example, Dang et al. (2012) produced monodispersed microparticles of PEGDA and poly(ethylene glycol) methyl ether acrylate

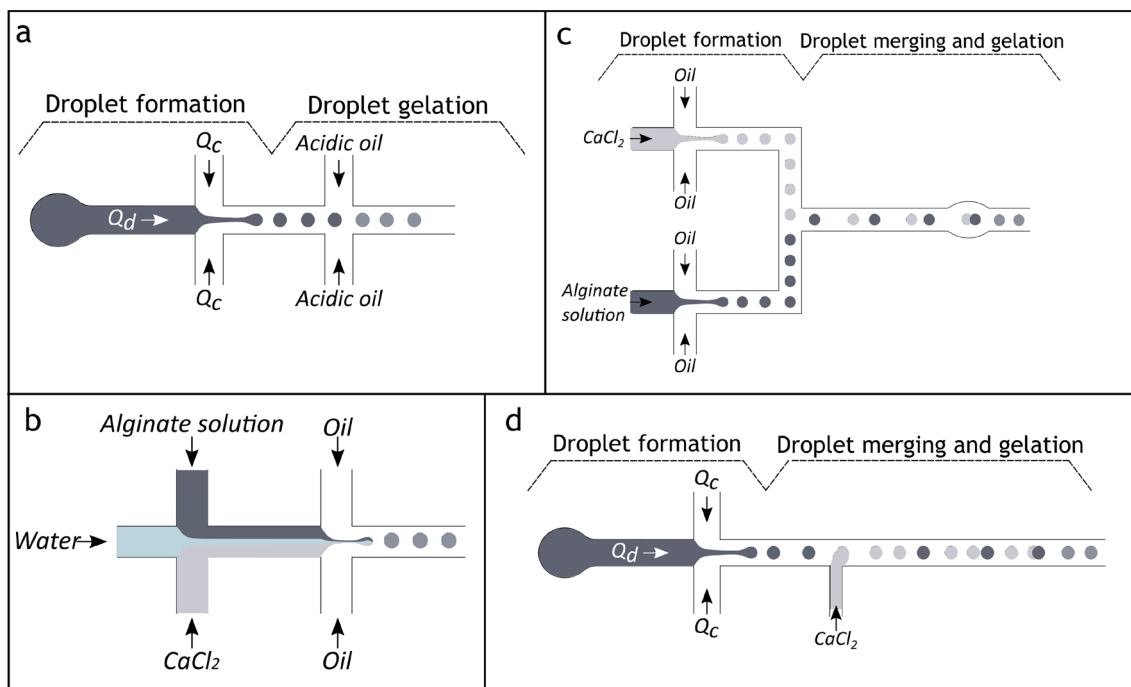


Fig. 9 Schemes used for alginate microparticle production: **a** use of acidic oil to induce pH gelation (Tan and Takeuchi 2007); **b** slow fusion of alginate and CaCl_2 droplets using a water layer to separate the two monomers (Mazutis et al. 2015); **c** fusion of alginate droplets

with CaCl_2 droplets, with an expansion zone to obtain disk-shaped microparticles (Liu et al. 2006); **d** fusion of alginate and CaCl_2 droplets (Shintaku et al. 2007)

Table 3 PEG microparticles production by photopolymerization in microfluidic devices

| Hydrogel | Continuous phase | Particle shape | Photoinitiator | Surfactant | Size (μm) | Channel width (μm) | References |
|---------------|------------------|--------------------------|---|---------------------------------------|------------------------|---------------------------------|----------------------|
| PEGDA | Mineral oil | Spheres, plugs and disks | 2-Hydroxy-2-methylpropiophenone, 2-hydroxy-4'-(2-hydroxyethoxy)-2-methylpropiophenone | Abil EM 90 (3% v/v) | 10.8 | 40 | (Hwang et al. 2008a) |
| PEGDA/PEG-MEA | Mineral oil | Spheres | 2-Hydroxy-2-methylpropiophenone | Octylphenoxypolyethoxyethanol (1 wt%) | 40–200 | 100 | (Dang et al. 2012) |
| PEGDA | Mineral oil | Spheres | 2-Hydroxy-2-methylpropiophenone | ABIL EM 90 (3% v/v) | 50 | 50 | (Lewis et al. 2010) |
| PEGDA | Hexadecane | Spheres | 2-Hydroxy-2-methyl-1-phenyl-propan-1-one | Span 80 (> 3 wt%) | 45–95 | 200 | (Choi et al. 2009) |
| PEGDA | Silicon oil | Spheres | 2-Hydroxy-2-methylpropiophenone | – | 75–375 | 75 | (Yu et al. 2013) |

(PEGMEA) using a microfluidic device and photopolymerization by UV irradiation. They studied the influence of the channel geometry, flow rates and hydrogel concentration. Lee et al. (2010b) produced PEGDA microgels for *E. coli* encapsulation by polymerization using a microfluidic device—Fig. 8d. Lewis et al. (2010) used a flow-focusing device to produce microparticles of viral nanotemplates in PEGDA—Fig. 8c and e. The viral nanotemplates were uniformly distributed through the PEGDA, while the droplets were polymerized by UV irradiation. Hwang et al. (2008a) produced spherical and non-spherical magnetic microgel particles using a microfluidic device and a UV light reflector. They used PEGDA and obtained monodispersed microparticles. The use of a UV light reflector contributed to improving the photopolymerization of the hydrogel.

The combination of droplet microfluidics with UV radiation has inherent limitations, as the range of geometries that can be produced is restricted to spheres, plugs or disks (Dendukuri et al. 2007). The alternative is to use photolithography, a method that enables the design on demand of the particle shape. The shape of the particle is defined by an optical mask that partially blocks the incident UV light (Dendukuri et al. 2007).

Photolithography requires that only a defined region of fluid is exposed to UV light for a short time. Since the target material is flowing in the microchannel, the high-throughput production of microparticles is an important challenge for photolithography. This problem is the motivation for the development of techniques to operate the microparticle production continuously:

1. Continuous flow lithography (CFL) (Dendukuri and Doyle 2009) takes advantage of the inhibition reaction

caused by the oxygen from the air diffusing through the polymer. This inhibition creates a barrier against the photopolymerization of the hydrogel near the wall, enabling the transport of microparticles through the microchannel. CFL must operate at a low flow rate otherwise the particles obtained will be smeared and will have a poor resolution.

2. Stop flow lithography (SFL) (Dendukuri et al. 2007; Dendukuri and Doyle 2009) can overcome the limitations of the CFL process. The flowing stream of the photopolymerizable hydrogel is stopped, and only then the UV light is turned on, improving the resolution of the microparticles.
3. Stop flow interference lithography (SFIL) (Dendukuri and Doyle 2009; Jang et al. 2007) enables the formation of microparticles with 3D characteristics. A phase mask that induces peaks into the light intensity and in the direction of propagation is used, enabling the control of the geometrical parameters and of the volume fraction of the microstructure formed.

Photolithography has led to the production of a large variety of particle shapes and functionalities. Hwang et al. (2008a) obtained disk, plug and sphere shape microparticles through photomasks—Fig. 10a–c. They noticed that the deformation of the microparticles can occur due to non-uniform UV light exposure and to large gradients of UV light. This problem was solved through the use of a UV light reflector made of aluminum foil. Zhan et al. (2002) produced PEG hydrogel parallelepipedic microparticles ($135 \mu\text{m} \times 200 \mu\text{m} \times 15 \mu\text{m}$) using photomasks in microchannels. The size of the microchannel and the size and shape of the photomask defined the size and shape of the microparticles.

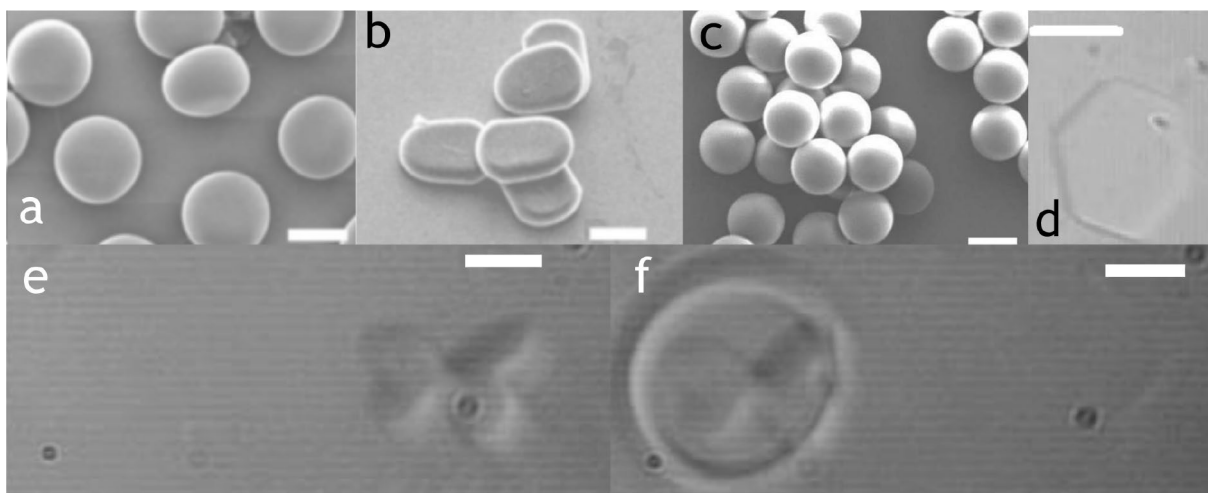


Fig. 10 Microparticles of PEG with different shapes obtained by photolithography: **a** disks; **b** plugs; **c** spheres; **d** hexagon; **e** butterfly; **f** butterfly and ring. Scale bars for **a–c** are of 20 μm and for **d–f** are of 100 μm . Images **a–c** Republished with permission of Royal Society of Chemistry (Great Britain) from Microfluidic-based synthesis of non-

spherical magnetic hydrogel microparticles, (Hwang et al. 2008b), 2020; permission conveyed through Copyt Clearance Center, Inc. While **d–f** Reprinted from (Chung et al. 2007), with the permission of AIP Publishing

It is also possible to use maskless lithography techniques. These techniques use spatial light modulators (SLMs) controlled by a computer (Chung et al. 2007). Chung et al. (2007) used an optofluidic maskless lithography process to obtain PEGDA microstructures. They were able to produce a butterfly and a ring microstructure (with approximately 150 μm length and 130 μm height)—Fig. 10d and e. This type of photolithographic method reduces the time and cost spent to generate the masks.

5 Hydrogel properties

Hydrogels can be produced from natural sources (natural hydrogels) or by chemical synthesis in laboratories (synthetic hydrogels) (Tumarkin and Kumacheva 2009; Gao et al. 2012a)—Table 4. Natural hydrogels present poor mechanical properties, but, due to their biocompatibility, have a high potential to interact directly with cells. Synthetic hydrogels present poor interaction with cells, but they have better mechanical properties and can be easily produced in large quantities. The selection of a hydrogel depends on the intended application. Due to their biocompatibility, agarose, alginate and poly(ethylene glycol), Pluronic F-127 and carrageenan are the most used hydrogels and their characteristics will be discussed in some detail.

To design a microfluidic setup for particle production, the fluids used need to be fully characterized. As shown in Sect. 2, in droplet microfluidics, the flow regime and the droplet size depend on the Capillary numbers of both phases and on the viscosity ratio. Droplet size is also influenced

Table 4 Natural and synthetic hydrogels

| Hydrogels | | |
|----------------------------------|-----------------------|--------------------------------------|
| Natural hydrogels | | Synthetic hydrogels |
| Proteins | Polysaccharides | |
| Collagen | Agarose | PEG—poly(ethylene glycol) |
| Gelatin | Alginate | PAC—poly(acrylic acid) |
| Fibrin | Chitosan | PVA—poly(vinyl alcohol) |
| Elastin-like polypeptides (ELPs) | Hyaluronic acid | Poloxamers |
| | Cellulose derivatives | pNiPAAm—poly(N-isopropyl acrylamide) |
| | Dextran | |
| | Xyloglucan | |
| | Carrageenan | |

by the surfactant concentration and interfacial tension. Depending on the gelation method, additional properties are required such as the gelation temperature and reactant concentration.

5.1 Properties of thermoreversible hydrogels

In microfluidics, the most commonly used thermoreversible hydrogels are agarose, Pluronic F-127, carrageenan and gelatine. Their gelation properties (Table 5) are critical to the design of the device and the setting of the operational conditions of the experimental setup. These properties include the melting temperature, the gelling temperature and the

Table 5 Physical properties of agarose, Pluronic F-127, gelatin and κ -carrageenan

| | Agarose | Pluronic F-127 | Gelatin | K-Carrageenan |
|----------------------------|---|---|---|--|
| Gelling temperature (°C) | 15–30 (Tumarkin and Kumacheva 2009; Leng et al. 2010) | 20–40* (Matthew et al. 2002) | < 25 (Yeh et al. 2013) | < 30 (Grenha et al. 2010) |
| Melting temperature (°C) | 56 (Leng et al. 2010) | 60 (Matthew et al. 2002) | > 25 (Yeh et al. 2013) | > 30 (Grenha et al. 2010) |
| Viscosity (Pa.s) | 0.5×10^{-2} (0.5% wt) (Kumachev et al. 2011) 2.4×10^{-1} (3.0% wt) (Kumachev et al. 2011) | ≈ 0.1 Pa.s (15% wt, 25°C) (Stoeber et al. 2005) | 1.35×10^{-3} (1% wt) (Park et al. 2016) 3.07×10^{-2} (30% wt) (Park et al. 2016) | 1.31×10^{-1} (15 g/L, 40°C) (Leong et al. 2011) |
| Interfacial tension (mN/m) | 2.2 (Kumachev et al. 2011; Oh et al. 2008) | 36 ± 0.29 (at 1% wt and 25°C) (Shah et al. 2015) | 4 (Aubry et al. 2015) | 7.08 (Leong et al. 2011) |
| Critical concentration | $0.065 \pm 0.005 \times 10^{-4}$ (mol/L) (high viscosity) $0.106 \pm 0.005 \times 10^{-4}$ (mol/L) (low viscosity) | 17–18% wt in water (Matthew et al. 2002) | - | - |

*Depending on the concentration

monomer critical concentration (minimum concentration of the hydrogel monomer required for gelation). The hydrogel needs to be in the liquid state when it is injected into the microchannel. After, the microdroplets need to be solidified by decreasing or increasing the temperature, depending on the hydrogel used. After gelation, the microparticles remain solid below its melting temperature, which, usually, does not coincide with its solidification temperature.

Agarose is a neutral polysaccharide extracted from seaweeds (Zamora-Mora et al. 2014a; Ellis and Jacquier 2009a) extensively used in biomedical research (Leng et al. 2010; Kumachev et al. 2011) and in the food industry (Ellis and Jacquier 2009a). The gelling temperature of agarose is in the range 15–30 °C (Tumarkin and Kumacheva 2009; Leng et al. 2010) and above this temperature, agarose is in the liquid state (Leng et al. 2010). Agarose gels will only change again to the liquid state when the temperature rises to its melting temperature (56 °C) (Leng et al. 2010). The correct design of the microfabrication procedure also needs to take into account the variability of agarose properties with concentration. According to Normand et al. (2000), the gelation temperature increases when agarose concentration increases. The authors also referred that agarose has a critical concentration below which gelation does not occur; this limit is 6.5×10^{-6} mol/L for high viscosity agarose and 1.06×10^{-5} mol/L for low viscosity agarose.

Pluronic F-127 is a copolymer (Yeh et al. 1996; Matthew et al. 2002; Geroski and Edelhofer 2000; Gilbert et al. 1987) with many applications since its gelation temperature (20–40 °C) is close to the human body temperature. Besides, Pluronic F-127 is non-toxic and so it can be easily employed in drug delivery systems (Giovagnoli et al. 2010; Nie et al. 2011). At low temperatures, Pluronic F-127 is a micellar liquid and when the temperature starts to increase, the micelles start to aggregate and pack forming a gel (Dumortier et al.

2006). The gelling temperature depends on the concentration, decreasing when the concentration increases (Matthew et al. 2002; Dumortier et al. 2006). A solution with a concentration between 20 and 30% (wt) can form a gel between 30 and 35 °C (Matthew et al. 2002). According to Matthew et al. (2002), the minimum concentration to form a gel is about 17–18% (wt) in water. Gilbert et al. (1987) studied the thermal gelation of Pluronic F-127. They concluded that at higher concentrations (24–34% wt), the gelling temperature is very low. Stoeber et al. (2005) studied Pluronic F-127 solutions (10–30% wt) and concluded that above 26 °C, the viscosity strongly increases. Stoeber et al. (2006) observed that Pluronic F-127 presents a shear-thinning behavior near the gelling point, however, at lower temperatures, it exhibits a Newtonian behavior.

The properties of Pluronic F-127 were explored by Aubry et al. (2015) to immobilize early larval *Caenorhabditis elegans* for visualization. The larvae were first isolated inside droplets of 25% (w/v) Pluronic F-127 solution formed at 12 °C in a microfluidic device. The droplets were then heated, by moving the device to a room at 22 °C, to entrap the larvae in solid Pluronic F-127. The authors selected 12 °C as the temperature of droplet formation, using a controlled chamber to avoid unstable flow conditions at temperatures near the gelling temperature.

Carrageenan (Leong et al. 2011; Grenha et al. 2010) is, like agarose, extracted from seaweeds and, depending on the method of extraction, different types of Carrageenan are obtained (Grenha et al. 2010). From all the carrageenan types, only κ -carrageenan and τ -carrageenan can form gels, being κ -carrageenan gels more rigid (Grenha et al. 2010). κ -Carrageenan gels form at low temperatures and turn into the liquid state when heated (Leong et al. 2011; Grenha et al. 2010; Ellis and Jacquier 2009b; Li et al. 2014). It can also form a gel in the presence of mono- and divalent cations

such as KCl, NaCl and $MgCl_2$ (Leong et al. 2011; Li et al. 2014).

Gelatine, another natural hydrogel, is suitable for medical and pharmaceutical applications due to its biocompatibility, biodegradability, non-toxicity and easy removal in physiological environment (Park et al. 2016; Yeh et al. 2013). Gelatine is thermoreversible and becomes a gel when the temperature decreases below 25 °C (for a solution of 1% (w/v)) (Yeh et al. 2013).

The properties of the microparticles are also very important, since for each application they should have specific characteristics. One of the most important is their integrity, i.e., the particles need to have good mechanical characteristics, otherwise can fragment. The mechanical properties are also important for the design of biomimetic fluids (e.g., blood analogue fluids). In the area of drug delivery, the cross-linking density and the diffusion coefficient are also very relevant, to control the drug release rate. A low cross-linking density will result in a rapid drug release.

Significant research has been dedicated to optimizing the conditions required to improve the mechanical properties of hydrogel particles, by testing different temperatures and composition and by experimenting hybrid materials. Kumachev et al. (2011) produced agarose microbeads by droplet microfluidic with different mechanical properties by modifying the agarose concentration and temperature. When they increased the concentration, the gel became stronger, since the elastic shear modulus increased: at 4 °C, agarose hydrogels with a concentration of 0.75% (wt) had an elastic shear modulus of 26 Pa while agarose hydrogels with a concentration of 3.0% (wt) had an elastic shear modulus of 4420 Pa. When they increased the temperature, the gel became weaker; when the temperature was increased to 37 °C, the elastic shear modulus for 0.75% (wt) and 3.0% (wt) decreased to 1 Pa and 700 Pa, respectively. They also concluded that a longer gelation time increases the rigidity of agarose microbeads. Zamora-Mora et al. (2014a) produced chitosan/agarose microparticles with controlled size using microfluidic emulsification. They concluded that chitosan offers a reinforcement of the gel structure, improving the mechanical properties of agarose. In addition, Park et al. (2016) concluded that, for gelatine microparticles, the increase in gelatine concentration led to the formation of strong networks and, by consequence, gel microparticles with better mechanical properties. Increasing the temperature, the microparticles stiffness decreases mostly due to the degradation of the polymer network.

5.2 Properties of ionic hydrogels

One of the most used hydrogels that undergo ionic gelation is alginate. Alginate is a linear copolymer also extracted from seaweeds composed of two acid monomers: β -D-mannuronic

acid and α -L-guluronic acid (Gao et al. 2012a; Choi et al. 2007; Xu et al. 2008; Tan and Takeuchi 2007). When alginate chains get into contact with multivalent cations such as Ca^{2+} , Ba^{2+} or Fe^{3+} , an alginate hydrogel is easily obtained (Gao et al. 2012a; Choi et al. 2007; Shintaku et al. 2006; Xu et al. 2008).

Alginate hydrogels can be formed by fast and easy methods (Mazutis et al. 2015; Choi et al. 2007; Xu et al. 2008) and also present a slow degradation rate (Mazutis et al. 2015). Alginate viscosity depends on the concentration of the solution while the interfacial tension depends on the specific surfactant and continuous phases used (Table 6). Viscoelastic and shear-thinning behaviors (Martinez et al. 2012) have been observed and viscosity is sensible to pH variations (Lee and Mooney 2012). Alginate concentration and the critical concentration of the cross-linker (minimum concentration of the reactive species to occur gelation) need to be specified and controlled during microparticle formation. Mazutis et al. (2015) produced biconcave alginate microparticles with a size similar to mammalian cells in a microfluidic device—Fig. 7. They concluded that above 2% (w/w) of alginate, the process is unfeasible due to the high viscosity of the solution. They also concluded that a concentration of $CaCl_2$ between 2 and 5% (w/w) leads to gelation before droplet formation, while a concentration of 0.1% (w/w) does not promote gelation. The most viable concentration range of $CaCl_2$ to produce droplets of alginate hydrogel is between 0.5 and 1.0% (w/w), for which gelation occurs after the droplet formation. Microbeads can be obtained by adding a surfactant to decrease the interfacial tension of the continuous phase.

For alginate hydrogels, the mechanical properties are determined by the sodium and alginate solution concentrations, cross-linking density and gelation rate of the hydrogel (LeRoux et al. 1999). An increase in the sodium and alginate solution concentrations leads to an increase in the viscosity and surface tension (Ye et al. 2017). The higher is the

Table 6 Properties of alginate

| Property | Value |
|--|----------------------|
| Viscosity (0.5% wt) (Pa.s) (Choi et al. 2007) | 4.0×10^{-2} |
| Viscosity (1.0% wt) (Pa.s) (Choi et al. 2007) | 8.0×10^{-2} |
| Viscosity (2.0% wt) (Pa.s) (Choi et al. 2007) | 2.4×10^{-1} |
| Surface tension (mN/m) (Shintaku et al. 2006) | 72 |
| Sodium alginate solution 1.5% (w/w) at 20 °C | |
| Interfacial tension (mN/m) (Shintaku et al. 2006) | 34 |
| Sodium alginate solution 1.5% (w/w) and food oil at 25 °C | |
| Density (g/cm^3) (Lee et al. 2000) | 0.8755 |
| Sodium alginate solution 2% (w/w) at 25 °C | |
| Minimum concentration of $CaCl_2$ to form hydrogel (w/w) (Mazutis et al. 2015) | 0.5% |

concentration of alginate the higher are compressive and shear moduli, while the concentration of Na^{2+} has the opposite effect (LeRoux et al. 1999). The mechanical strength of alginate hydrogel decreases when it is exposed to physiological environments (Lee et al. 2000; LeRoux et al. 1999). (Benavides et al. 2012) studied the effect of CaCO_3 concentration on the mechanical properties of alginate hydrogels. They concluded that, in the presence of CaCO_3 , the mechanical strength of the hydrogels improved due to the development of a rigid network, originated by the interactions between the alginate and calcium ions. The gelation rate of alginate hydrogels also influences the final mechanical properties. Kuo and Ma (2001) concluded that a slow gelation rate results in better mechanical properties. The mechanical properties of alginate hydrogels are summarized in Table 7.

5.3 Properties of photopolymerizable hydrogels

The most used synthetic photopolymerizable hydrogels are poly(ethylene glycol) derivatives such as PEG acrylate and PEG methacrylate derivatives (Nguyen and West 2002). PEG hydrogels are bio-inert (Gao et al. 2012a; An et al. 2009), can easily incorporate bioactive and biodegradable species (Gao et al. 2012a), are non-toxic (Lee et al. 2010b; An et al. 2009), hydrophilic (An et al. 2009; Rossow et al. 2012) and can resist to cell and protein adhesion and absorption (An et al. 2009), the reason why they are immune and resist to inflammatory processes (Gao et al. 2012a; An et al. 2009). PEG was approved by the Food and Drug Administration (FDA) for oral and dermal applications (Xue et al. 2014; Evans et al. 2014).

The production of microparticles by photopolymerization has additional constraints and new additional parameters

Table 7 Mechanical properties of alginate hydrogels

| Property | Value |
|---|---|
| Maximum shear modulus (kPa) (Lee et al. 2000) (gel formed with an alginate solution of 2% (w/w)) | 24.4 ± 0.6 |
| Tensile strength (MPa) (Benavides et al. 2012) (film of hydrogel formed with an alginate solution of 1.5% (w/v), addition of glycerol as plasticizer) | 39.7 ± 5.3 (0 g CaCO ₃ /g alginate) 52.6 ± 6.1 (0.01 g CaCO ₃ /g alginate) 51.9 ± 5.8 (0.02 g CaCO ₃ /g alginate) 52.9 ± 5.5 (0.03 g CaCO ₃ /g alginate) |
| Percent of elongation (%) (Benavides et al. 2012) (film of hydrogel formed with an alginate solution of 1.5% (w/v), addition of glycerol as a plasticizer) | 4.4 ± 0.5 (0 g CaCO ₃ /g alginate) 4.5 ± 0.8 (0.01 g CaCO ₃ /g alginate) 2.3 ± 1.2 (0.02 g CaCO ₃ /g alginate) 2.3 ± 0.9 (0.03 g CaCO ₃ /g alginate) |
| Dynamic shear modulus (kPa) (LeRoux and M., F. Guilak, and L. Setton, 1999) (gel formed with an alginate solution of 2% (w/w)) | 23.57 ± 5.91 |
| Young Modulus (kPa) (Chan et al. 2011) (gel formed with an alginate solution of 15 g/L and CaCl ₂ = 0.5 M) | 339 |

need to be known, namely: the photoinitiator concentration, hydrogel monomer concentration, UV light intensity, wavelength and exposure time. When PEG acrylate and PEG methacrylate derivatives are exposed to UV light in the presence of a photoinitiator, the photoinitiator dissociates and creates radicals that attack the carbon–carbon double bond of the acrylate, triggering a free radical polymerization (An et al. 2009). Filatov et al. (2017) performed a study to obtain the gelation time and the mechanical properties of PEGDA microparticles. They concluded that the gelation time is strongly dependent on the photoinitiator concentration and that SPAN 80 influences the solidification of the particles (comparison with the absence of surfactant and with the use of Abil EM 180). They obtained an optimal value for the photoinitiator concentration around 1% (w/w). Table 8 summarizes the key physical properties of the poly(ethylene glycol) diacrylate.

The monomer concentration influences the cross-linking density, which determines the microparticle mechanical properties. Allazetta et al. (2013) produced PEG hydrogels with different cross-linking densities by varying PEG concentration. Duprat et al. (2015) developed a method to measure the elastic modulus of PEGDA microparticles produced in a microfluidic device and showed that the elastic modulus increases with the increase of PEG concentration and exposure time. The diffusion of solutes in hydrogels can be estimated by optical and elution methods. Evans et al. (2014) used a microfluidic device, optical and elution methods and effluent analysis to estimate the solute diffusion in PEG hydrogels. They concluded that with high polymer concentrations, the hydrogel becomes more cross-linked and the diffusion coefficients are smaller.

Merkel et al. (2011) used 2-hydroxyethylacrylate combined with PEGDA to reproduce red blood cells. The objective was to obtain particles with properties (size, shape and deformability) similar to those of red blood cells. They concluded that the cross-linking density strongly influences the mechanical properties of the microparticles. With a cross-linking density of 10%, they obtained an elastic modulus of 63.9 kPa, while for a cross-linking density of 1% the modulus was 7.8 kPa. The elastic modulus of the red blood cells (RBCs) is 26 ± 7 kPa (Tomaiuolo 2014), indicating that PEGDA can be used to mimic the RBCs by tuning the concentration.

Poly(vinyl alcohol) (PVA) derivatives and hyaluronic acid (HA) derivatives are also photopolymerizable (Nguyen and West 2002). Poly(vinyl alcohol) has good mechanical properties and demonstrates good optical and elastic properties (Kityk et al. 1997; Schmedlen et al. 2002). PVA is biocompatible and resists to protein adsorption and cell adhesion and has properties suitable for drug delivery (Schmedlen et al. 2002). Schmedlen et al. (2002) concluded that the elastic modulus and ultimate tensile strength of PVA hydrogels increase with an increase of the PVA concentration. Hyaluronic acid is a natural hydrogel found in the human body (Burdick et al. 2005; Burdick and Prestwich 2011). Hyaluronic acid solutions have high viscosity and shear-thinning behavior (Schanté et al. 2011). Due to its biocompatibility, hyaluronic acid has many applications and can be used in drug delivery systems and eye surgeries (Burdick and Prestwich 2011; Schanté et al. 2011).

6 Control of size, shape and microstructure

Particles produced by droplet microfluidics are spherical by default, but other shapes can be obtained by modifying the technique. Cylindrical particles can be obtained if the gelation is carried out when the particles are confined along axisymmetric microchannels (Cai et al. 2019). Double-emulsion techniques are used to obtain core and shell (Yu et al. 2019) and Janus particles (Geng et al. 2018) comprising different materials. Spherical microparticles can be combined in clusters of different arrangements to produce colloidal molecules (Shen et al. 2016). However, more complex shapes require photolithography. By selecting the appropriate mask shape, it is possible to produce planar particles of any shape and even composite particles of different materials (Dendukuri and Doyle 2009; Dendukuri et al. 2007).

In droplet microfluidics, the size of the particle produced depends on the size of the microchannel and on the operational conditions that determine the flow regime. In the dripping regime, the particle is usually larger than the channel width, while in the jetting regime the particle can be much smaller than the channel width (see works listed in Tables 1, 2, 3). Depending on the flow rate ratio (Cubaud and Mason 2008), the size of the particles can be 25% of the channel width (Cubaud and Mason 2008; Carneiro et al. 2019).

Table 8 Physical properties of the poly(ethylene glycol) diacrylate

| Property | Value |
|---------------------------------------|--|
| Viscosity (10% wt) | 2.2×10^{-2} (Pa.s) (Ziemecka et al. 2011) |
| Surface tension (10% wt) | 0.1 (mN/m) (Ziemecka et al. 2011) |
| Critical surfactant concentration—wt% | > 3 (PEGDA 95% wt) (Choi et al. 2009) |
| Critical surfactant concentration—wt% | 1 (PEGDA 50% wt) (Yousefi et al. 1997) |

Practical limits restrict the size, and size distribution, of the particles that can be produced by droplet microfluidics. To operate in the dripping regime, the Capillary number of the dispersed phase must be smaller than the critical value, 0.1, which implies that $\mu\nu$ must be smaller than 0.1σ . Therefore, to operate in the dripping regime, the flow rate has an upper threshold, which is lower when the viscosity of the dispersed phase is higher. In addition, viscous fluids lead to high pressures in the device, restricting the size of the channel that can be used for the same throughput.

Photolithography is an alternative to droplet microfluidics for two main reasons: the fabrication accuracy is higher and the range of shapes that can be produced is wider. Photolithography can produce structures of 400 nm on a stationary polymer precursor (Nakagawa et al. 1990). In the case of two-photon laser writing, the particles can have 200 nm and the accuracy of the technique can reach 20 nm. However, to achieve high throughput, the production needs to operate in a continuous flow, which reduces the accuracy of the method. Furthermore, if the liquid precursor flows too fast, the particles can be distorted by the velocity gradients in the flow. Stop and flow techniques (Dendukuri et al. 2007; Dendukuri and Doyle 2009) have been developed to address this problem, but the stop/flow process is difficult to control and some smear of the particles can still be observed at high flow velocities. Full 3D particles, with detailed features and high throughput, can be obtained by moving the light source to offset the flow distortion (Shaw et al. 2018).

7 Challenges and future developments

The production of hydrogel microparticles through microfluidic systems presents several advantages, such as control over the size and shape of the droplets, control over the consumption of reactants, control over the timing of the reactions and the ability to conduct reactions with high efficiency under safe conditions. Although all these advantages, some issues need to be studied and developed further.

Cell encapsulation and drug delivery systems can be used for several therapies, such as diabetes, bone and cartilage injuries, heart diseases and cancer. Hydrogel microparticles in these therapies require the removal of the continuous phase from the particles. If the continuous phase is not completely removed, contamination of the microparticles may trigger an immune response of the human body (Gao et al. 2012a). In addition, it is still not possible to encapsulate precisely only one cell per droplet, which has been and will be a challenge (Tumarkin and Kumacheva 2009).

In chemical reactors, hydrogel microparticles promote higher reaction rates due to their higher surface-to-volume ratio (Teh et al. 2008). However, there is a chance that the molecular adsorption at the microparticles interferes with

the reaction when the reaction rate is too high. Extreme reaction conditions can damage the hydrogel microparticles and this can also be a challenge for several applications (Teh et al. 2008).

Photolithographic techniques have had significant progress in recent years. It is now possible to produce 3D particles with 3D features and submicrometric accuracy. The field is now ready to address new challenges. The most prominent is the scale-up of the microparticles production and the development of new applications for which microparticles with 3D features are relevant. The most promising approach to scale-up is parallelization, which, in the case of photolithography, requires the parallelization of the optical equipment. The integration of the optical equipment in the microdevice, using optofluidic (Fan and White 2011; Schmidt and Hawkins 2008) miniaturization fabrication method is a route that needs to be explored. New applications need to be developed for microparticles with 3D features. Among the most promising are the use of particles as components of more complex structures and machines (Chung et al. 2008; Sacanna et al. 2010; Wang et al. 2014). Particles could also be used as lock and key devices for selective interactions with biological species.

Hydrogels are responsive to temperature and pH variations and so they are suitable for actuator functions (Ionov 2014; Ma et al. 2018). The responsiveness of hydrogels can also be explored to develop swimmers suitable to operate as microbots (Magdanz et al. 2014; Jeon and Hayward 2017). Anisotropic particles are also suitable for the development of microbots (Palacci et al. 2015) and fluids with anisotropic viscosity. Microfabrication techniques able to produce particles of any shape and of different materials can be combined with the manipulation of the particle environment to obtain microbots able to perform medical roles, like complex drug delivery operations in specific spots of the human body.

The particle output of a microfluidic device is in the range of microliters per minute, which limits significantly the amount of particles that can be produced using a single microfluidic device. The flow rate of the dispersed phase is limited by the high-pressure drop and the maximum pressure the device can support. Furthermore, to obtain monodispersed particles, the system must operate in the dripping regime, and so this limit is even lower. The amount of particles that can be produced is also constrained by the viscosity of the dispersed phase. Therefore, high-throughput microfluidic systems are only feasible by scale-up through parallelization (Tumarkin and Kumacheva 2009). But parallelization itself has also its issues. Parallel devices are based on hierarchical networks prone to feedback effects and chaotic flow patterns, which lead to the formation of polydispersed microparticles. Two types of networks are usually used, tree configurations and ladder configurations. Ladder configurations generate more stable flows, while in tree configurations

the flow is sensitive to small microfabrication defects (Tetradis-Meris et al. 2009).

To be effective, parallelization needs to have a 3D arrangement, leading to new design and fabrication challenges. Recently, femtosecond laser micromachining has been used to produce 3D microstructures (Maia et al. 2017; Liao et al. 2012) and the technique is suitable for the fabrication of 3D networks with integrated waveguides (Maia et al. 2017), facilitating the integration of optical components for high-throughput photolithography.

Control of the mechanical properties of the hydrogels to extend their range of applicability is also a topic that requires further developments. The mechanical properties of the hydrogel microparticles can be improved by the introduction of new materials in their cross-linked structure. Carbon nanotubes are one of the promising materials to improve hydrogel mechanical properties (Kawaguchi et al. 2006). More complex structures, such as micro-vascularized networks, can be obtained with the use of 3D microfluidic platforms (Chung et al. 2012).

One significant challenge is the use of hydrogel microparticles as oxygen carriers (Kimelman-Bleich et al. 2009; Wijekoon et al. 2013). Hydrogels need to be combined with perfluorocarbons or hemoglobin to produce particles that can carry high quantities of oxygen. Production and rheology of the particles and blood analogues need to be optimized. This approach may contribute to the development of blood substitutes for disease treatments and tissue engineering without the ethical limitations of actual blood.

8 Conclusions

This review describes the most important aspects of the production of hydrogel microparticles through microfluidic devices. These devices enable the control of the size, shape and mechanical properties of the hydrogel microparticles. Several routes are available for particle fabrication in microfluidic devices. The properties of the precursor fluids and the definition of the operating conditions are crucial for the design of the microfluidic device, mainly because they determine the flow regimes and the droplet sizes. Surfactants should be carefully chosen to assure that the droplets do not coalesce before the solidification step. The surfactants distribution can have complex interactions with the flow patterns influencing the particle size.

Complex particle shapes can be produced by photolithography. However, to increase the throughput, the device needs to operate in continuous flow. Methods to achieve this, by synchronizing the UV radiation emission with the flow, and compensating distortions due to the fluid flow, were reviewed. Presently, the available technologies can

produce, in principle, any particle shape with submicrometric accuracy.

The hydrogel microparticles have a great potential in several biomedical applications, and the use of microfluidics enables precise control over the formation of the particles and is useful to overcome most of the specific needs of these applications. Significant challenges remain yet to use microfluidics for large-scale particle production.

Acknowledgements This work was funded by FEDER funds through COMPETE2020—Operational Programme for Competitiveness Factors (POCI) and National Funds (PIDDAC) through FCT (Fundação para a Ciência e a Tecnologia) under project POCI-01-0145-FEDER-016861-PTDC/QEQ-FTT/4287/2014, PhD grant PD/BD/114313/2016 and Transport Phenomena Research Center—CEFT base funding UIDB/00532/2020.

Data availability Data sharing not applicable—no new data generated.

References

- Ahmadi R, de Bruijn JD (2008) Biocompatibility and gelation of chitosan-glycerol phosphate hydrogels. *J Biomed Mater Res A* 86(3):824–832
- Akbari S, Pirbodaghi T (2013) Microfluidic encapsulation of cells in alginate particles via an improved internal gelation approach. *Microfluid Nanofluid* 16(4):773–777
- Allazetta S, Hausherr TC, Lutolf MP (2013) Microfluidic synthesis of cell-type-specific artificial extracellular matrix hydrogels. *Biomacromol* 14(4):1122–1131
- An SY, Bui MP, Nam YJ, Han KN, Li CA, Choo J, Lee EK, Katoh S, Kumada Y, Seong GH (2009) Preparation of monodisperse and size-controlled poly(ethylene glycol) hydrogel nanoparticles using liposome templates. *J Colloid Interface Sci* 331(1):98–103
- Anna SL, Mayer HC (2006) Microscale tipstreaming in a microfluidic flow focusing device. *Phys Fluids* 18(12):1215–1218
- Aubry G, Zhan M, Lu H (2015) Hydrogel-droplet microfluidic platform for high-resolution imaging and sorting of early larval *Caenorhabditis elegans*. *Lab Chip* 15(6):1424–1431
- Baret JC (2012) Surfactants in droplet-based microfluidics. *Lab Chip* 12(3):422–433
- Baret JC, Kleinschmidt F, El Harrak A, Griffiths AD (2009) Kinetic aspects of emulsion stabilization by surfactants: a microfluidic analysis. *Langmuir* 25(11):6088–6093
- Baroud CN, Willaime H (2004) Multiphase flows in microfluidics. *C R Phys* 5(5):547–555
- Baroud CN, Delville JP, Gallaire F, Wunenburger R (2007) Thermocapillary valve for droplet production and sorting. *Phys Rev E Stat Nonlin Soft Matter Phys* 75(4 Pt 2):046302
- Baroud CN, Gallaire F, Dangler R (2010) Dynamics of microfluidic droplets. *Lab Chip* 10(16):2032–2045
- Benavides S, Villalobos-Carvajal R, Reyes JE (2012) Physical, mechanical and antibacterial properties of alginate film: effect of the crosslinking degree and oregano essential oil concentration. *J Food Eng* 110(2):232–239
- Benmekhbi M, Simon S, Sjöblom J (2014) Dynamic and rheological properties of span 80 at liquid-liquid interfaces. *J Dispersion Sci Technol* 35(6):765–776

- Brenker JC, Collins DJ, Van Phan H, Alan T, Neild A (2016) On-chip droplet production regimes using surface acoustic waves. *Lab Chip* 16(9):1675–1683
- Burdick JA, Prestwich GD (2011) Hyaluronic acid hydrogels for biomedical applications. *Adv Mater* 23(12):H41–56
- Burdick JA, Chung C, Jia X, Randolph MA, Langer R (2005) Controlled degradation and mechanical behavior of photopolymerized hyaluronic acid networks. *Biomacromol* 6(1):386–391
- Cai Q-W, Ju X-J, Chen C, Faraj Y, Jia Z-H, Hu J-Q, Xie R, Wang W, Liu Z, Chu L-Y (2019) Fabrication and flow characteristics of monodisperse bullet-shaped microparticles with controllable structures. *Chem Eng J* 370:925–937
- Carneiro J, Doutel E, Campos JBLM, Miranda JM (2016) PDMS droplet formation and characterization by hydrodynamic flow focusing technique in a PDMS square microchannel. *J Micro-mech Microeng* 26(10):105013
- Carneiro J, Campos JBLM, Miranda JM (2019) PDMS microparticles produced in PDMS microchannels under the jetting regime for optimal optical suspensions. *Coll Surf Physicochem Eng Aspects* 580:123737
- Cellesi F, Weber W, Fussenegger M, Hubbell JA, Tirelli N (2004) Towards a fully synthetic substitute of alginate: optimization of a thermal gelation/chemical cross-linking scheme (“tandem” gelation) for the production of beads and liquid-core capsules. *Biotechnol Bioeng* 88(6):740–749
- Cerdeira ATS, Campos J, Miranda JM, Araujo JDP (2020) Review on microbubbles and microdroplets flowing through microfluidic geometrical elements. *Micromachines (Basel)* 11:2
- Chan E-S, Lim T-K, Voo W-P, Pogaku R, Tey BT, Zhang Z (2011) Effect of formulation of alginate beads on their mechanical behavior and stiffness. *Particuology* 9(3):228–234
- Chen JZ, Troian SM, Darhuber AA, Wagner S (2005) Effect of contact angle hysteresis on thermocapillary droplet actuation. *J Appl Phys* 97(1):014906
- Choi C-H, Jung J-H, Rhee YW, Kim D-P, Shim S-E, Lee C-S (2007) Generation of monodisperse alginate microbeads and in situ encapsulation of cell in microfluidic device. *Biomed Micro-device* 9(6):855–862
- Choi C-H, Jung J-H, Hwang T-S, Lee C-S (2009) In situ microfluidic synthesis of monodisperse PEG microspheres. *Macromol Res* 17(3):163–167
- Christopher GF, Anna SL (2007) Microfluidic methods for generating continuous droplet streams. *J Phys D Appl Phys* 40(19):R319–R336
- Chuah AM, Kuroiwa T, Kobayashi I, Zhang X, Nakajima M (2009) Preparation of uniformly sized alginate microspheres using the novel combined methods of microchannel emulsification and external gelation. *Colloids Surf, A* 351(1):9–17
- Chung SE, Park W, Park H, Yu K, Park N, Kwon S (2007) Optofluidic maskless lithography system for real-time synthesis of photopolymerized microstructures in microfluidic channels. *Appl Phys Lett* 91(4):041106
- Chung SE, Park W, Shin S, Lee SA, Kwon S (2008) Guided and fluidic self-assembly of microstructures using railed microfluidic channels. *Nat Mater* 7(7):581
- Chung BG, Lee KH, Khademhosseini A, Lee SH (2012) Microfluidic fabrication of microengineered hydrogels and their application in tissue engineering. *Lab Chip* 12(1):45–59
- Cubaud T, Mason TG (2008) Capillary threads and viscous droplets in square microchannels. *Phys Fluids* 20(5):053302
- Dang T-D, Kim YH, Kim HG, Kim GM (2012) Preparation of monodisperse PEG hydrogel microparticles using a microfluidic flow-focusing device. *J Ind Eng Chem* 18(4):1308–1313
- Darhuber AA, Valentino JP, Troian SM, Wagner S (2003) Thermocapillary actuation of droplets on chemically patterned surfaces by programmable microheater arrays. *J Microelectromech Syst* 12(6):873–879
- del Campo A, Greiner C (2007) SU-8: a photoresist for high-aspect-ratio and 3D submicron lithography. *J Micromech Microeng* 17(6):R81
- Dendukuri D, Doyle PS (2009) The synthesis and assembly of polymeric microparticles using microfluidics. *Adv Mater* 21(41):4071–4086
- Dendukuri D, Gu SS, Pregibon DC, Hatton TA, Doyle PS (2007) Stop-flow lithography in a microfluidic device. *Lab Chip* 7(7):818–828
- Destgeer G, Sung HJ (2015) Recent advances in microfluidic actuation and micro-object manipulation via surface acoustic waves. *Lab Chip* 15(13):2722–2738
- Duffy DC, McDonald JC, Schueller OJ, Whitesides GM (1998) Rapid Prototyping of Microfluidic Systems in Poly(dimethylsiloxane). *Anal Chem* 70(23):4974–4984
- Dumortier G, Grossiord JL, Agnely F, Chaumeil JC (2006) A review of poloxamer 407 pharmaceutical and pharmacological characteristics. *Pharm Res* 23(12):2709–2728
- Duprat C, Berthel H, Wexler JS, du Roure O, Lindner A (2015) Microfluidic in situ mechanical testing of photopolymerized gels. *Lab Chip* 15(1):244–252
- Ellis A, Jacquier JC (2009a) Manufacture and characterisation of agarose microparticles. *J Food Eng* 90(2):141–145
- Ellis A, Jacquier JC (2009b) Manufacture of food grade κ -carrageenan microspheres. *J Food Eng* 94(3):316–320
- Evans SM, Litzemberger AL, Ellenberger AE, Maneval JE, Jablonski EL, Vogel BM (2014) A microfluidic method to measure small molecule diffusion in hydrogels. *Mater Sci Eng C Mater Biol Appl* 35:322–334
- Fan X, White IM (2011) Optofluidic microsystems for chemical and biological analysis. *Nat Photonics* 5(10):591
- Farn RJ (2008) Chemistry and technology of surfactants. Wiley, Blackwell Publishing Ltd, Oxford (UK)
- Filatov NA, Nozdriukhin DV, Bukatin AS (2017) The kinetic study of solidification PEGDA microparticles in flow-focusing microfluidic chip. *J Phys: Conf Ser* 917(4):042024
- Fischer P, Erni P (2007) Emulsion drops in external flow fields—the role of liquid interfaces. *Curr Opin Colloid Interface Sci* 12(4–5):196–205
- Friend J, Yeo L (2010) Fabrication of microfluidic devices using polydimethylsiloxane. *Biomicrofluidics* 4(2):026502
- Gao A, Liu X, Li T, Gao X, Wang Y (2012a) Thermocapillary Actuation of Droplets on a Microfluidic Chip. *J Adhes Sci Technol* 26(12–17):2165–2176
- Gao A, Liu X, Li T, Gao X, and Wang Y (2012b) Thermocapillary actuation of droplets on a microfluidic chip. *J Adhes Sci Technol ahead-of-print(ahead-of-print)* 26(12–17):2165–2176
- Geng Y-H, Ge X-H, Zhang S-B, Zhou Y-W, Wang Z-Q, Chen J, Xu J-H (2018) Microfluidic preparation of flexible micro-grippers with precise delivery function. *Lab Chip* 18(13):1838–1843
- Geroski DH, Edelhauser HF (2000) Drug delivery for posterior segment eye disease. *Invest Ophthalmol Vis Sci* 41(5):961–964
- Gilbert JC, Richardson JL, Davies MC, Palin KJ, Hadgraft J (1987) The effect of solutes and polymers on the gelation properties of pluronic F-127 solutions for controlled drug delivery. *J Control Release* 5(2):113–118
- Giovagnoli S, Tsai T, DeLuca PP (2010) Formulation and release behavior of doxycycline-alginate hydrogel microparticles embedded into pluronic F127 thermogels as a potential new vehicle for doxycycline intradermal sustained delivery. *AAPS PharmSciTech* 11(1):212–220
- Gong J, Kim CJ (2008) All-electronic droplet generation on-chip with real-time feedback control for EWOD digital microfluidics. *Lab Chip* 8(6):898–906

- Grenha A, Gomes ME, Rodrigues M, Santo VE, Mano JF, Neves NM, Reis RL (2010) Development of new chitosan/carrageenan nanoparticles for drug delivery applications. *J Biomed Mater Res A* 92(4):1265–1272
- Hoare TR, Kohane DS (2008) Hydrogels in drug delivery: progress and challenges. *Polymer* 49(8):1993–2007
- Huang J, Hastings CL, Duffy GP, Kelly HM, Raeburn J, Adams DJ, Heise A (2013) Supramolecular hydrogels with reverse thermal gelation properties from (oligo)tyrosine containing block copolymers. *Biomacromol* 14(1):200–206
- Hwang DK, Dendukuri D, Doyle PS (2008) Microfluidic-based synthesis of non-spherical magnetic hydrogel microparticles. *Lab Chip* 8(10):1640–1647
- Ionov L (2014) Hydrogel-based actuators: possibilities and limitations. *Mater Today* 17(10):494–503
- Jagur-Grodzinski J (2009) Polymeric gels and hydrogels for biomedical and pharmaceutical applications. *Poly Adv Technol* 21:1 (p. n/a-n/a)
- Jang JH, Dendukuri D, Hatton TA, Thomas EL, Doyle PS (2007) A route to three-dimensional structures in a microfluidic device: stop-flow interference lithography. *Angew Chem Int Ed* 46(47):9027–9031
- Jegannathan KR, Chan E-S, Ravindra P (2009) Physical and stability characteristics of *Burkholderia cepacia* lipase encapsulated in κ -carrageenan. *J Mol Catal B Enzym* 58(1):78–83
- Jeon SJ, Hayward RC (2017) Reconfigurable microscale frameworks from concatenated helices with controlled chirality. *Adv Mater* 29(17):1606111
- Jeong W-W, Kim C (2011) One-step method for monodisperse microgels by glass capillary microfluidics. *Colloids Surf, A* 384(1–3):268–273
- Jeong WC, Lim JM, Choi JH, Kim JH, Lee YJ, Kim SH, Lee G, Kim JD, Yi GR, Yang SM (2012) Controlled generation of submicron emulsion droplets via highly stable tip-streaming mode in microfluidic devices. *Lab Chip* 12(8):1446–1453
- Jo S, Kim J, Kim SW (2006) Reverse thermal gelation of aliphatically modified biodegradable triblock copolymers. *Macromol Biosci* 6(11):923–928
- Jones TB, Gunji M, Washizu M, Feldman MJ (2001) Dielectrophoretic liquid actuation and nanodroplet formation. *J Appl Phys* 89(2):1441–1448
- Joo MK, Sohn YS, Jeong B (2007) Stereoisomeric effect on reverse thermal gelation of poly(ethylene glycol)/poly(lactide) multi-block copolymer. *Macromolecules* 40(14):5111–5115
- Kawaguchi M, Fukushima T, Hayakawa T, Nakashima N, Inoue Y, Takeda S, Okamura K, Taniguchi K (2006) Preparation of carbon nanotube-alginate nanocomposite gel for tissue engineering. *Dent Mater J* 25(4):719–725
- Khademhosseini A, Langer R (2007) Microengineered hydrogels for tissue engineering. *Biomaterials* 28(34):5087–5092
- Kimelman-Bleich N, Pelled G, Sheyn D, Kallai I, Zilberman Y, Mizrahi O, Tal Y, Tawackoli W, Gazit Z, Gazit D (2009) The use of a synthetic oxygen carrier-enriched hydrogel to enhance mesenchymal stem cell-based bone formation in vivo. *Biomaterials* 30(27):4639–4648
- Kityk IV, Kasperczyk J, Sahraoui B, Yasinskii MF, Holan B (1997) Low temperature anomalies in polyvinyl alcohol photopolymers. *Polymer* 38(19):4803–4806
- Klouda L, Mikos AG (2008) Thermoresponsive hydrogels in biomedical applications. *Eur J Pharm Biopharm* 68(1):34–45
- Kumachev A, Greener J, Tumarkin E, Eiser E, Zandstra PW, Kumacheva E (2011) High-throughput generation of hydrogel microbeads with varying elasticity for cell encapsulation. *Biomaterials* 32(6):1477–1483
- Kuo C, Ma P (2001) Ionically crosslinked alginate hydrogels as scaffolds for tissue engineering: part 1. *Struct Gelat Rate Mech Propert* 22:511–521
- Lee KY, Mooney DJ (2012) Alginate: properties and biomedical applications. *Prog Polym Sci* 37(1):106–126
- Lee KY, Rowley JA, Eiselt P, Moy EM, Bouhadir KH, Mooney DJ (2000) Controlling mechanical and swelling properties of alginate hydrogels independently by cross-linker type and cross-linking density. *Macromolecules* 33(11):4291–4294
- Lee JN, Park C, Whitesides GM (2003) Solvent compatibility of poly(dimethylsiloxane)-based microfluidic devices. *Anal Chem* 75(23):6544–6554
- Lee W, Walker LM, Anna SL (2009) Role of geometry and fluid properties in droplet and thread formation processes in planar flow focusing. *Phys Fluids* 21(3):032103
- Lee KG, Park TJ, Soo SY, Wang KW, Kim BI, Park JH, Lee CS, Kim DH, Lee SJ (2010) Synthesis and utilization of *E. coli*-encapsulated PEG-based microdroplet using a microfluidic chip for biological application. *Biotechnol Bioeng* 107(4):747–751
- Lee KG, Park TJ, Soo SY, Wang KW, Kim BII, Park JH, Lee C-S, Kim DH, Lee SJ (2010) Synthesis and utilization of *E. coli*-encapsulated PEG-based microdroplet using a microfluidic chip for biological application. *Biotechnol Bioeng* 107(4):747–751
- Leng X, Zhang W, Wang C, Cui L, Yang CJ (2010) Agarose droplet microfluidics for highly parallel and efficient single molecule emulsion PCR. *Lab Chip* 10(21):2841–2843
- Leong J-Y, Lim T-K, Pogaku R, Chan E-S (2011) Size prediction of κ -carrageenan droplets formed in co-flowing immiscible liquid. *Particuology* 9(6):637–643
- Leong J-Y, Lam W-H, Ho K-W, Voo W-P, Lee MF-X, Lim H-P, Lim S-L, Tey B-T, Poncelet D, Chan E-S (2016) Advances in fabricating spherical alginate hydrogels with controlled particle designs by ionotropic gelation as encapsulation systems. *Particuology* 24:44–60
- LeRoux AM, Guilak F, Setton L (1999) Compressive and shear properties of alginate gel: effects of sodium ions and alginate concentration. *J Biomed Mater Res* 47:46–53
- Lewis CL, Lin Y, Yang C, Manocchi AK, Yuet KP, Doyle PS, Yi H (2010) Microfluidic fabrication of hydrogel microparticles containing functionalized viral nanotemplates. *Langmuir* 26(16):13436–13441
- Li L, Ni R, Shao Y, Mao S (2014) Carrageenan and its applications in drug delivery. *Carbohydr Polym* 103:1–11 (Supplement C)
- Liao Y, Song J, Li E, Luo Y, Shen Y, Chen D, Cheng Y, Xu Z, Sugioka K, Midorikawa K (2012) Rapid prototyping of three-dimensional microfluidic mixers in glass by femtosecond laser direct writing. *Lab Chip* 12(4):746–749
- Lin H-H, Cheng Y-L (2001) In-Situ Thermoreversible Gelation of Block and Star Copolymers of Poly(ethylene glycol) and Poly(N-isopropylacrylamide) of Varying Architectures. *Macromolecules* 34(11):3710–3715
- Liu K, Ding HJ, Liu J, Chen Y, Zhao XZ (2006) Shape-controlled production of biodegradable calcium alginate gel microparticles using a novel microfluidic device. *Langmuir* 22(22):9453–9457
- Liu Y, Geever LM, Kennedy JE, Higginbotham CL, Cahill PA, McGuinness GB (2010) Thermal behavior and mechanical properties of physically crosslinked PVA/Gelatin hydrogels. *J Mech Behav Biomed Mater* 3(2):203–209
- Liu K, Deng Y, Zhang N, Li S, Ding H, Guo F, Liu W, Guo S, Zhao X-Z (2012) Generation of disk-like hydrogel beads for cell encapsulation and manipulation using a droplet-based microfluidic device. *Microfluid Nanofluid* 13(5):761–767
- Lorenz H, Despont M, Fahrni N, LaBianca N, Renaud P, Vettiger P (1997) SU-8: a low-cost negative resist for MEMS. *J Micromech Microeng* 7(3):121

- Ma C, Lu W, Yang X, He J, Le X, Wang L, Zhang J, Serpe MJ, Huang Y, Chen T (2018) Bioinspired anisotropic hydrogel actuators with on-off switchable and color-tunable fluorescence behaviors. *Adv Func Mater* 28(7):1704568
- Magdanz V, Stoychev G, Ionov L, Sanchez S, Schmidt OG (2014) Stimuli-Responsive Microjets with Reconfigurable Shape. *Angew Chem Int Ed* 53(10):2673–2677
- Maia JM, Amorim VA, Alexandre D, Marques PV (2017) Real-time optical monitoring of etching reaction of microfluidic channel fabricated by femtosecond laser direct writing. *J Lightwave Technol* 35(11):2291–2298
- Martinez CJ, Kim JW, Ye C, Ortiz I, Rowat AC, Marquez M, Weitz D (2012) A microfluidic approach to encapsulate living cells in uniform alginate hydrogel microparticles. *Macromol Biosci* 12(7):946–951
- Mata A, Fleischman AJ, Roy S (2005) Characterization of polydimethylsiloxane (PDMS) properties for biomedical micro/nanosystems. *Biomed Microdevices* 7(4):281–293
- Matthew JE, Nazario YL, Roberts SC, Bhatia SR (2002) Effect of mammalian cell culture medium on the gelation properties of Pluronic® F127. *Biomaterials* 23(23):4615–4619
- Mazutis L, Griffiths AD (2012) Selective droplet coalescence using microfluidic systems. *Lab Chip* 12(10):1800–1806
- Mazutis L, Vasiliauskas R, Weitz DA (2015) Microfluidic production of alginate hydrogel particles for antibody encapsulation and release. *Macromol Biosci* 15(12):1641–1646
- McClements DJ, Henson L, Popplewell LM, Decker EA, Choi SJ (2012) Inhibition of Ostwald ripening in model beverage emulsions by addition of poorly water soluble triglyceride oils. *J Food Sci* 77(1):C33–C38
- McDonald JC, Whitesides GM (2002) Poly(dimethylsiloxane) as a material for fabricating microfluidic devices. *Acc Chem Res* 35(7):491–499
- McDonald JC, Duffy DC, Anderson JR, Chiu DT, Wu H, Schueller OJ, Whitesides GM (2000) Fabrication of microfluidic systems in poly(dimethylsiloxane). *Electrophoresis* 21(1):27–40
- Merkel TJ, Jones SW, Herlihy KP, Kersey FR, Shields AR, Napier M et al (2011) Using mechanobiological mimicry of red blood cells to extend circulation times of hydrogel microparticles. *Proc Natl Acad Sci U S A* 108(2):586–591
- Myers D (2005) Surfactant science and technology. In: John Wiley & Sons (eds) Inc, New Jersey
- Nakagawa K, Taguchi M, Ema T (1990) Fabrication of 64 M DRAM with i-line phase-shift lithography. *Int Tech Digest Elect Dev IEEE*. <https://doi.org/10.1109/IETDM.1990.237037>
- Natarajan S, Chang-Yen D, Gale B (2008) Large-area, high-aspect-ratio SU-8 molds for the fabrication of PDMS microfluidic devices. *J Micromech Microeng* 18(4):045021
- Nelson WC, Kim CJC (2012) Droplet actuation by electrowetting-on-dielectric (EWOD): a review. *J Adhes Sci Technol ahead-of-print*(ahead-of-print): 26(12–17):1747–1771
- Nguyen KT, West JL (2002) Photopolymerizable hydrogels for tissue engineering applications. *Biomaterials* 23(22):4307–4314
- Nie S, Hsiao WL, Pan W, Yang Z (2011) Thermoreversible Pluronic F127-based hydrogel containing liposomes for the controlled delivery of paclitaxel: in vitro drug release, cell cytotoxicity, and uptake studies. *Int J Nanomedicine* 6:151–166
- Nishinari K, Watase M (1987) Effects of polyhydric alcohols on thermal and rheological properties of polysaccharide gels. *Agric Biol Chem* 51(12):3231–3238
- Normand V, Lootens DL, Amici E, Plucknett KP, Aymard P (2000) New insight into agarose gel mechanical properties. *Biomacromol* 1(4):730–738
- Oberti S, Neild A, Quach R, Dual J (2009) The use of acoustic radiation forces to position particles within fluid droplets. *Ultrasonics* 49(1):47–52
- Oh JK, Drumright R, Siegwart DJ, Matyjaszewski K (2008) The development of microgels/nanogels for drug delivery applications. *Prog Polym Sci* 33(4):448–477
- Oliveira MB, Mano JF (2011) Polymer-based microparticles in tissue engineering and regenerative medicine. *Biotechnol Prog* 27(4):897–912
- Palacci J, Sacanna S, Abramian A, Barral J, Hanson K, Grosberg AY, Pine DJ, Chaikin PM (2015) Artificial rheotaxis. *Sci Adv* 1(4):e1400214
- Park D, Wu W, Wang Y (2011) A functionalizable reverse thermal gel based on a polyurethane/PEG block copolymer. *Biomaterials* 32(3):777–786
- Park K-S, Kim C, Nam J-O, Kang S-M, Lee C-S (2016) Synthesis and characterization of thermosensitive gelatin hydrogel microspheres in a microfluidic system. *Macromol Res* 24(6):529–536
- Patel MA, AbouGhaly MH, Schryer-Praga JV, Chadwick K (2017) The effect of ionotropic gelation residence time on alginate cross-linking and properties. *Carbohydr Polym* 155:362–371
- Patil J, Kamalapur MV, Marapur SC, Kadam DV (2010) Ionotropic gelation and polyelectrolyte complexation: The novel techniques to design hydrogel particulate sustained, modulated drug delivery system. *Rev* 5(1):241–248
- Patil P, Chavanke D, Wagh MA (2012) A review on ionotropic gelation method: Novel approach for controlled *gastroretentive gelspheres*. *Int J Pharm Pharm Sci* 4:27–32
- Pensado A, Fernandez-Pineiro I, Seijo B, Sanchez A (2014) Anionic nanoparticles based on Span 80 as low-cost, simple and efficient non-viral gene-transfection systems. *Int J Pharm* 476(1–2):23–30
- Perez Bravo JJ, Francois N (2016) Chitosan-starch beads prepared by ionotropic gelation as potential matrices for controlled release of fertilizers. *Carbohydr Polym* 148:134–142
- Pethig R (2010) Review article-dielectrophoresis: status of the theory, technology, and applications. *Biomicrofluidics* 4(2):022811
- Petka WA, Harden JL, McGrath KP, Wirtz D, Tirrell DA (1998) Reversible hydrogels from self-assembling artificial proteins. *Science* 281(5375):389–392
- Pochan DJ, Schneider JP, Kretsinger J, Ozbas B, Rajagopal K, Haines L (2003) Thermally reversible hydrogels via intramolecular folding and consequent self-assembly of a de novo designed peptide. *J Am Chem Soc* 125(39):11802–11803
- Ré M-I (2006) Formulating drug delivery systems by spray drying. *Drying Technol* 24(4):433–446
- Rossov T, Heyman JA, Ehrlicher AJ, Langhoff A, Weitz DA, Haag R, Seiffert S (2012) Controlled synthesis of cell-laden microgels by radical-free gelation in droplet microfluidics. *J Am Chem Soc* 134(10):4983–4989
- Sacanna S, Irvine WT, Chaikin PM, Pine DJ (2010) Lock and key colloids. *Nature* 464(7288):575
- Sacco P, Paoletti S, Cok M, Asaro F, Abrami M, Grassi M, Donati I (2016) Insight into the ionotropic gelation of chitosan using triphosphosphate and pyrophosphate as cross-linkers. *Int J Biol Macromol* 92:476–483
- Sakai S, Ito S, Inagaki H, Hirose K, Matsuyama T, Taya M, Kawakami K (2011) Cell-enclosing gelatin-based microcapsule production for tissue engineering using a microfluidic flow-focusing system. *Biomicrofluidics* 5(1):13402
- Samanipour R, Wang Z, Ahmadi A, Kim K (2015) Experimental and computational study of microfluidic flow-focusing generation of gelatin methacrylate hydrogel droplets. *J Appl Poly Sci* 133:29
- Say-Hwa T, Nam-Trung N, Levent Y, Tae Goo K (2010) Formation and manipulation of ferrofluid droplets at a microfluidic T-junction. *J Micromech Microeng* 20(4):045004
- Schanté CE, Zuber G, Herlin C, Vandamme TF (2011) Chemical modifications of hyaluronic acid for the synthesis of derivatives for a broad range of biomedical applications. *Carbohydr Polym* 85(3):469–489

- Schmedlen RH, Masters KS, West JL (2002) Photocrosslinkable polyvinyl alcohol hydrogels that can be modified with cell adhesion peptides for use in tissue engineering. *Biomaterials* 23(22):4325–4332
- Schmid L, Franke T (2014) Acoustic modulation of droplet size in a T-junction. *Appl Phys Lett* 104(13):133501
- Schmidt H, Hawkins AR (2008) Optofluidic waveguides: I. Conc Implement *Microfluid Nanofluid* 4(1–2):3–16
- Shah V, Bharatiya B, Shah DO, Mukherjee T (2015) Correlation of dynamic surface tension with sedimentation of PTFE particles and water penetration in powders. *Langmuir* 31(51):13725–13733
- Sharma S, Srisa-Art M, Scott S, Asthana A, Cass A (2013) Droplet-Based Microfluidics. In: Jenkins G, Mansfield CD (eds) *Microfluidic diagnostics: methods and protocols*. Humana Press, Totowa, NJ, pp 207–230
- Shaw LA, Chizari S, Shusteff M, Naghsh-Nilchi H, Di Carlo D, Hopkins JB (2018) Scanning two-photon continuous flow lithography for synthesis of high-resolution 3D microparticles. *Opt Express* 26(10):13543–13548
- Shen B, Ricouvier J, Malloggi F, Tabeling P (2016) Designing colloidal molecules with microfluidics. *Adv Sci* 3(6):1600012
- Shintaku H, Kuwabara T, Kawano S, Suzuki T, Kanno I, Kotera H (2006) Micro cell encapsulation and its hydrogel-beads production using microfluidic device. *Microsyst Technol* 13(8–10):951–958
- Shintaku H, Kuwabara T, Kawano S, Suzuki T, Kanno I, Kotera H (2007) Micro cell encapsulation and its hydrogel-beads production using microfluidic device. *Microsyst Technol* 13(8):951–958
- Stoeber B, Zhihao Y, Liepmann D, Muller SJ (2005) Flow control in microdevices using thermally responsive triblock copolymers. *J Microelectromech Syst* 14(2):207–213
- Stoeber B, Hu C-MJ, Liepmann D, Muller SJ (2006) Passive flow control in microdevices using thermally responsive polymer solutions. *Phys Fluids* 18(5):053103
- Sung Kwon C, Hyejin M, Chang-Jin K (2003) Creating, transporting, cutting, and merging liquid droplets by electrowetting-based actuation for digital microfluidic circuits. *J Microelectromech Syst* 12(1):70–80
- Tan WH, Takeuchi S (2007) Monodisperse alginate hydrogel microbeads for cell encapsulation. *Adv Mater* 19(18):2696–2701
- Teh S-Y, Lin R, Hung L-H, Lee AP (2008) Droplet microfluidics. *Lab Chip* 8(2):198–220
- Tetradis-Meris G, Rossetti D, Pulido de Torres CN, Cao R, Lian G, Janes R (2009) Novel parallel integration of microfluidic device network for emulsion formation. *Indust Eng Chem Res* 48(19):8881–8889
- Todd PL, Jon FE (2013) A review of the theory, methods and recent applications of high-throughput single-cell droplet microfluidics. *J Phys D Appl Phys* 46(11):114005
- Tomaiuolo G (2014) Biomechanical properties of red blood cells in health and disease towards microfluidics. *Biomicrofluidics* 8(5):051501
- Tostado CP, Xu J, Luo G (2011) The effects of hydrophilic surfactant concentration and flow ratio on dynamic wetting in a T-junction microfluidic device. *Chem Eng J* 171(3):1340–1347
- Tsuchiya H, Okochi M, Nagao N, Shikida M, Honda H (2008) On-chip polymerase chain reaction microdevice employing a magnetic droplet-manipulation system. *Sensors Actuat Chem* 130(2):583–588
- Tumarkin E, Kumacheva E (2009) Microfluidic generation of microgels from synthetic and natural polymers. *Chem Soc Rev* 38(8):2161–2168
- Um E, Lee D-S, Pyo H-B, Park J-K (2008) Continuous generation of hydrogel beads and encapsulation of biological materials using a microfluidic droplet-merging channel. *Microfluid Nanofluid* 5(4):541–549
- Utada A, Lorenceau E, Link D, Kaplan P, Stone HA, Weitz D (2005) Monodisperse double emulsions generated from a microcapillary device. *Science* 308(5721):537–541
- Wang Y, Wang Y, Zheng X, Yi G-R, Sacanna S, Pine DJ, Weck M (2014) Three-dimensional lock and key colloids. *J Am Chem Soc* 136(19):6866–6869
- Wassén S, Rondeau E, Sott K, Lorén N, Fischer P, Hermansson A-M (2012) Microfluidic production of monodisperse biopolymer particles with reproducible morphology by kinetic control. *Food Hydrocolloids* 28(1):20–27
- Wehking JD, Chew L, Kumar R (2013) Droplet deformation and manipulation in an electrified microfluidic channel. *Appl Phys Lett* 103(5):054101
- Weng L, Zhang L, Ruan D, Shi L, Xu J (2004) Thermal gelation of cellulose in a NaOH/thiourea aqueous solution. *Langmuir* 20(6):2086–2093
- Wijekoon A, Fountas-Davis N, Leipzig ND (2013) Fluorinated methacrylamide chitosan hydrogel systems as adaptable oxygen carriers for wound healing. *Acta Biomater* 9(3):5653–5664
- Wixforth A, Strobl C, Gauer C, Toegl A, Scriba J, Guttenberg ZV (2004) Acoustic manipulation of small droplets. *Anal Bioanal Chem* 379(7–8):982–991
- Wooster TJ, Golding M, Sanguansri P (2008) Impact of oil type on nanoemulsion formation and Ostwald ripening stability. *Langmuir* 24(22):12758–12765
- Xu JH, Li SW, Tan J, Luo GS (2008) Controllable preparation of monodispersed calcium alginate microbeads in a novel microfluidic system. *Chem Eng Technol* 31(8):1223–1226
- Xu Q, Hashimoto M, Dang TT, Hoare T, Kohane DS, Whitesides GM, Langer R, Anderson DG (2009) Preparation of monodisperse biodegradable polymer microparticles using a microfluidic flow-focusing device for controlled drug delivery. *Small* 5(13):1575–1581
- Xu JH, Dong PF, Zhao H, Tostado CP, Luo GS (2012) The dynamic effects of surfactants on droplet formation in coaxial microfluidic devices. *Langmuir* 28(25):9250–9258
- Xue P, Wu Y, Menon NV, Kang Y (2014) Microfluidic synthesis of monodisperse PEGDA microbeads for sustained release of 5-fluorouracil. *Microfluid Nanofluid* 18(2):333–342
- Yang C-G, Xu Z-R, Wang J-H (2010) Manipulation of droplets in microfluidic systems. *TrAC, Trends Anal Chem* 29(2):141–157
- Ye B, Xu H, Bao B, Xuan J, Zhang L (2017) 3D-printed air-blast microfluidic nozzles for preparing calcium alginate microparticles. *RSC Adv* 7(77):48826–48834
- Yeh MK, Davis SS, Coombes AGA (1996) Improving protein delivery from microparticles using blends of poly(DL lactide co-glycolide) and poly(ethylene oxide)-poly(propylene oxide) copolymers. *Pharm Res* 13(11):1693–1698
- Yeh C-H, Chen K-R, Lin Y-C (2013) Developing heatable microfluidic chip to generate gelatin emulsions and microcapsules. *Microfluid Nanofluid* 15(6):775–784
- Yin N, Stilwell MD, Santos TMA, Wang H, Weibel DB (2015) Agarose particle-templated porous bacterial cellulose and its application in cartilage growth in vitro. *Acta Biomater* 12:129–138
- Yizhong W, Yuejun Z, Sung Kwon C (2017) Efficient in-droplet separation of magnetic particles for digital microfluidics. *J Micro-mech Microeng* 17(10):2148
- Yousefi A, Laffleur PG, Gauvin R (1997) Kinetic studies of thermoset cure reactions: a review. *Polym Compos* 18(2):157–168
- Yu B, Cong H, Liu X, Ren Y, Wang J, Zhang L, Tang J, Ma Y, Akasaka T (2013) Preparation of monodisperse PEG hydrogel composite microspheres via microfluidic chip with rounded channels. *J Micromech Microeng* 23:095016

- Yu L, Sun Q, Hui Y, Seth A, Petrovsky N, Zhao C-X (2019) Microfluidic formation of core-shell alginate microparticles for protein encapsulation and controlled release. *J Colloid Interface Sci* 539:497–503
- Zamora-Mora V, Velasco D, Hernández R, Mijangos C, Kumacheva E (2014) Chitosan/agarose hydrogels: cooperative properties and microfluidic preparation. *Carbohydr Polym* 111:348–355
- Zamora-Mora V, Velasco D, Hernandez R, Mijangos C, Kumacheva E (2014a) Chitosan/agarose hydrogels: cooperative properties and microfluidic preparation. *Carbohydr Polym* 111:348–355
- Zhan W, Seong GH, Crooks RM (2002) Hydrogel-based microreactors as a functional component of microfluidic systems. *Anal Chem* 74(18):4647–4652
- Zhang Y, Nguyen NT (2017) Magnetic digital microfluidics: a review. *Lab Chip* 17(6):994–1008
- Zhang X, Li L, Luo C (2016) Gel integration for microfluidic applications. *Lab Chip* 16(10):1757–1776
- Zhu P, Kong T, Kang Z, Tian X, Wang L (2015) Tip-multi-breaking in capillary microfluidic devices. *Sci Rep* 5:11102
- Ziemecka I, van Steijn V, Koper GJ, Rosso M, Brizard AM, van Esch JH, Kreutzer MT (2011) Monodisperse hydrogel microspheres by forced droplet formation in aqueous two-phase systems. *Lab Chip* 11(4):620–624

Publisher's Note Springer Nature remains neutral with regard to jurisdictional claims in published maps and institutional affiliations.